Journal of Medicinal Chemistry Article

J. Med. Chem. **2009,** *52,* 4743–4756 **4743**
DOI: 10.1021/jm900166t

9-(Arenethenyl)purines as Dual Src/Abl Kinase Inhibitors Targeting the Inactive Conformation: Design, Synthesis, and Biological Evaluation

Wei-Sheng Huang,*[,†] Xiaotian Zhu,[†] Yihan Wang,[†] Mohammad Azam,[‡] David Wen,[†] Raji Sundaramoorthi,[†] R. Mathew Thomas,[†] Shuangying Liu,[†] Geetha Banda,[†] Scott P. Lentini,[†] Sasmita Das,[†] Qihong Xu,[†] Jeff Keats,[†] Frank Wang,[†] Scott Wardwell,[†] Yaoyu Ning,[†] Joseph T. Snodgrass,[†] Marc I. Broudy,[†] Karin Russian,[†] George Q. Daley,[‡] John Iuliucci,[†] David C. Dalgarno,[†] Tim Clackson,[†] Tomi K. Sawyer,[†] and William C. Shakespeare[†]

[†]*ARIAD Pharmaceuticals, Inc., 26 Landsdowne Street, Cambridge, Massachusetts 02139, and* [‡]*Department of Biological Chemistry and Molecular Pharmacology, Harvard Medical School, Division of Hematology/Oncology, Brigham and Women's Hospital, Dana-Farber Cancer Institute, and Division of Hematology/Oncology, The Children's Hospital, 300 Longwood Avenue, Boston, Massachusetts 02115*

Received February 9, 2009

A novel series of potent dual Src/Abl kinase inhibitors based on a 9-(arenethenyl)purine core has been identified. Unlike traditional dual Src/Abl inhibitors targeting the active enzyme conformation, these inhibitors bind to the inactive, DFG-out conformation of both kinases. Extensive SAR studies led to the discovery of potent and orally bioavailable inhibitors, some of which demonstrated in vivo efficacy. Once-daily oral administration of inhibitor **9i** (AP24226) significantly prolonged the survival of mice injected intravenously with wild type Bcr-Abl expressing Ba/F3 cells at a dose of 10 mg/kg. In a separate model, oral administration of **9i** to mice bearing subcutaneous xenografts of Src Y527F expressing NIH 3T3 cells elicited dose-dependent tumor shrinkage with complete tumor regression observed at the highest dose. Notably, several inhibitors (e.g., **14a**, AP24163) exhibited modest cellular potency (IC_{50} = 300−400 nM) against the Bcr-Abl mutant T315I, a variant resistant to all currently marketed therapies for chronic myeloid leukemia.

Introduction

Chronic myeloid leukemia (CML[a]) is characterized by a reciprocal translocation between chromosome 9 and 22, resulting in the short Philadelphia (Ph) chromosome[1] carrying the Bcr-Abl (Breakpoint cluster region−Abelson leukemia) oncogene.[2] This oncogene encodes the chimeric Bcr-Abl fusion protein, which incorporates an activated Abl tyrosine kinase domain and is responsible for the initial phase of CML.[3] In 2001, imatinib, a potent Bcr-Abl inhibitor, was approved for the treatment of CML.[4] Despite its tremendous clinical success, imatinib is relatively ineffective against advanced phases of CML and Philadelphia chromosome-positive acute lymphoblastic leukemia (Ph+ ALL).[5] Mutations in the kinase domain of Bcr-Abl are the major mechanism of acquired imatinib resistance.[6] To date, at least 50 different point mutations that encode distinct single amino acid substitutions have been identified in CML patients who are resistant to imatinib. Most mutants are effectively inhibited with second-generation inhibitors dasatinib and nilotinib, although neither compound inhibits the T315I mutant, which represents ~15−20% of all clinically observed mutants. Currently, there are no approved pharmaceutical therapies for CML patients harboring this mutation, and development of T315I targeted inhibitors addresses a significant unmet medical need.

Although the most widely accepted mechanism for imatinib resistance is the presence of kinase domain mutations, several studies have provided a rationale for the use of dual Src/Abl kinase inhibitors to overcome imatinib resistance.[7] For example, overexpression of Src family kinases (SFK) has recently been implicated in Bcr-Abl mediated leukemogenesis, particularly the induction of B-cell acute lymphoblastic leukemia (B-ALL), and also in CML disease progression.[8] Beyond CML, a recent study demonstrated endogenous Abl kinases (c-Abl and Arg) are activated by deregulated EGFR and Src kinases, driving invasion of aggressive breast cancer cells[9] and further highlighting the potential expanded utility of dual Src/Abl inhibitors to this solid tumor indication.[10] Moreover, Src activation or overexpression itself has been demonstrated in a variety of human tumor types, including colon, breast, pancreas, lung, liver, brain, and bladder cancers.[11] Taken together, dual Src/Abl kinase inhibitors, targeting either kinase independently or simultaneously, possess significant therapeutic potential for the treatment of both solid and hematologic malignancies. In 2006, dasatinib, a potent dual Src/Abl inhibitor, was approved for the treatment of adults in all phase of CML with resistance or intolerance to imatinib,[12] and there are now multiple dual Src/Abl kinase inhibitors in

*To whom correspondence should be addressed. Phone: 617-621-2341. Fax: 617-494-8144. E-mail: wei-sheng.huang@ariad.com.

[a] Abbreviations: CML, chronic myeloid leukemia; Bcr-Abl, breakpoint cluster region-abelson; Ph+ ALL, Philadelphia chromosome-positive acute lymphoblastic leukemia; Src/Abl, sarcoma /abelson; SFK, Src family kinases; B-ALL, B-cell acute lymphoblastic leukemia; Arg, Abl-related gene; EGFR, epidermal growth factor receptor; Lck, leukocyte-specific protein tyrosine kinase; c-Kit, cytokine receptor; PDGF, platelet-derived growth factor; P-loop: phosphate binding loop; ATP, adenosine-5′-triphosphate; DFG, aspartic acid-phenylalanine-glycine; VEGFR, vascular endothelial growth factor receptor; MAP, mitogen-activated protein; KDR, kinase insert domain receptor; PK, pharmacokinetic; WT, wild type.

Published on Web 07/02/2009

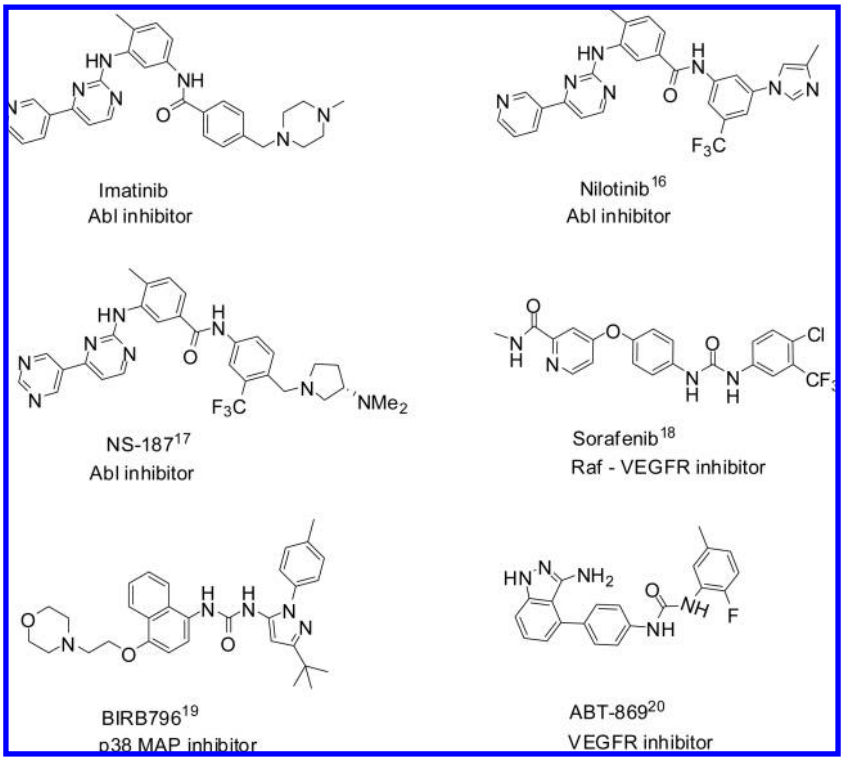

Figure 1. Representative kinase inhibitors targeting the DFG-out conformation.

clinical trials for the treatment of breast cancer, pancreatic cancer, and other solid tumors.[13]

Imatinib is a relatively selective kinase inhibitor. Prior to a recent study demonstrating modest Lck inhibition ($IC_{50} = 160$ nM),[14] imatinib was found to inhibit only three kinases: Bcr-Abl, c-Kit, and the PDGF receptor.[4] The high degree of kinase selectivity exhibited by imatinib is, to a large extent, attributed to its binding to the inactive conformation of Abl. In this conformation, the glycine rich P-loop folds down over the ATP binding site and the activation loop adopts a conformation in which it occludes substrate binding and disrupts the ATP binding site, blocking the catalytic activity of the enzyme.[15a] This binding mode induces changes in the orientation of the conserved Asp-Phe-Gly (DFG)-motif at the base of the activation loop in which the phenylalanine residue moves more than 10 Å from its position in the active conformation; the inactive conformation is therefore also termed the "DFG-out" conformation. The DFG-out conformation creates an additional hydrophobic pocket adjacent to the ATP pocket. The amino acids surrounding this pocket are less conserved relative to those in the ATP binding pocket, which may explain why inhibitors bound to this conformation of the protein usually exhibit more focused kinase selectivity.[15b] The chemical structure of imatinib and several other inhibitors targeting the DFG-out conformation of Abl and other important kinases are depicted in Figure 1.

Previously, we have described **1** (AP23464, Figure 2) as a purine-based, ATP-competitive, dual Src/Abl inhibitor that potently inhibits Src, wild type Bcr-Abl and a panel of Bcr-Abl mutants (except T315I) with subnanomolar potencies.[21] To further probe the purine core as a template for potent dual Src/Abl inhibitors, alternate 2-atom linkers between the template and a pendant hydrophobic substituent were explored. On the basis of this concept, two parallel programs were established targeting the "DFG-in" and "DFG-out" conformations of

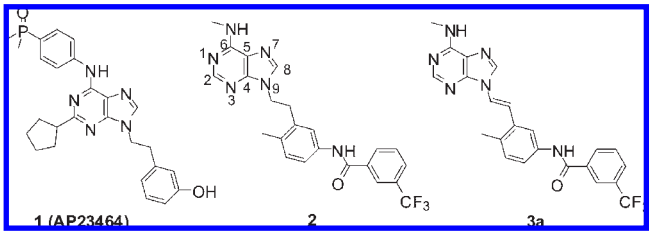

Figure 2. Design of DFG-out dual Src/Abl inhibitors based on **1**.

both proteins. Recently, we have reported progress on the "DFG-in" targeted inhibitors highlighting an N-9 vinyl linkage in a series of stable, synthetically accessible purine based dual Src/Abl inhibitors.[22] Herein we describe our work based on the same template but targeting the "DFG-out" conformation of both proteins.

Inhibitor Design

To transform **1** into a compound targeting the DFG-out conformations of Src and Abl, we initially used Abl as the primary target and proposed molecules **2** and **3a** (Figure 2), with the N^9-hydroxyphenethyl moiety being replaced by a privileged DFG-out targeting structural fragment, diarylamide.[23] Crystal structures of several "DFG-out" bound inhibitors have revealed that the amide functional group forms crucial hydrogen bonds with the protein and that the aryl groups fill adjacent hydrophobic pockets. Compound **3a** shares the 9-(arenethenyl)purine scaffold that was initially designed for our "DFG-in" dual Src/Abl inhibitor series and can also be viewed as conformationally restricted analogue of **2**. To investigate the molecular interactions between these inhibitors and Abl kinase, both compounds were docked into an Abl model based on the DFG-out conformation to which imatinib binds (PDB: 1iep). Side chains around the ligand site

were allowed to relax by using induced fit protocol in the Schrodinger modeling package.[24] The docked structure reveals that inhibitor **2** forms four hydrogen bonds with the protein. Two H-bonds are formed between the kinase hinge region and N-7 of purine core and methylamino group at C-1, respectively. The amide group of compound **2** forms two additional H-bonds with the side chain of Glu286 in the αC-helix and main chain of Asp381 in the DFG motif, respectively. The trifluoromethylphenyl moiety (B ring) fills a hydrophobic pocket that is only available in the DFG-out conformation. Extensive van der Waals (vdw) interactions are observed between the trifluoromethyl group and a small pocket formed by residue Ile293, Leu298, Leu354, and Val379. These vdw contacts between the trifluoromethyl group and the protein have been highlighted in the design of other DFG-out kinase inhibitors such as Abl inhibitors nilotinib, NS-187 (Figure 1),[17] and the dual Raf-KDR inhibitor sorafenib. Compound **3a** is predicted to bind to Abl in an identical mode to that of **2**, except that the olefinic proton (β to purine N-9) can potentially form a nonclassic hydrogen bond with the OH group of the Thr315 gatekeeper residue (Figure 3). Overall, inhibitors **2** and **3a** were predicted to interact with Abl in the DFG-out, inactive conformation, analogously to imatinib and nilotinib. The cyclopentyl group at purine C-2 in **1**, which was orientated toward the ribose-binding pocket of the ATP site,[25] was not accommodated in a DFG-out targeted inhibitor due to clashes with residues located in the glycine-rich P-loop (such as Leu248 and Tyr 253). In fact, the docking model suggested that the space therein was too tight to tolerate a group/atom larger than a proton. As such, our DFG-out targeted dual Src/Abl inhibitors would bear substituents at the 6,9-positions on the purine template as opposed to the traditional 2,6,9-trisubstitution.

Chemical Synthesis

We postulated that inhibitor **2** could be easily accessed by simple hydrogenation of **3a**, and so the synthesis of the latter compound became our primary objective. The synthetic approach to 9-(arenethenyl)purine **3** described in the literature is based on the Horner−Wadsworth−Emmons (HWE) reaction of N^9-(phosphorylmethyl)purine and substituted benzaldehydes.[26] This method was employed in the initial phase of our "DFG-in" inhibitor program but presented several challenges in the preparation of "DFG-out" targeted compounds because the corresponding elaborated benzaldehyde could only be made via a lengthy chemical transformation sequence. Other inconveniences included a multistep synthesis of the requisite HWE reagent and the separation of *Z*- and *E*-isomeric products. To circumvent these problems, we have developed an efficient synthesis of **3** based on a Heck reaction of 9-vinylpurines and aryl halides.[27] As shown in Scheme 1, 6-chloro-9-vinylpurine (**4**), prepared by direct vinylation of commercially available 6-chloropurine with excessive vinyl acetate in the presence of catalytic amount of sulfuric acid and mercury acetate,[28] underwent S_NAr displacement by aliphatic amines or palladium-catalyzed *N*-arylation with aryl amines to yield 6-(aryl/alkyl)amino-9-vinylpurines **5**. Subsequent Heck reaction of **5** and iodobenzamide **6**, which was prepared by a standard condensation of requisite acid and aniline, furnished **3** in high yields and exclusively as the *E*-isomers. Inhibitors **3a**, **3b**, **3g**, and **3h** (Table 1) were prepared in this manner, and subsequent hydrogenation of **3a** furnished **2** quantitatively.

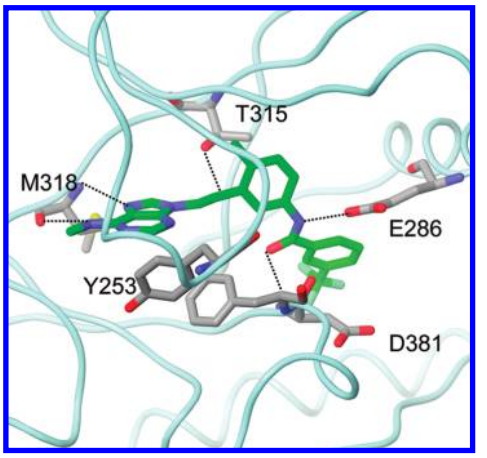

Figure 3. Model of designed inhibitor **3a** bound to Abl kinase

Scheme 1. Preparation of 3-(Trifluoromethyl)benzamides **3**[a]

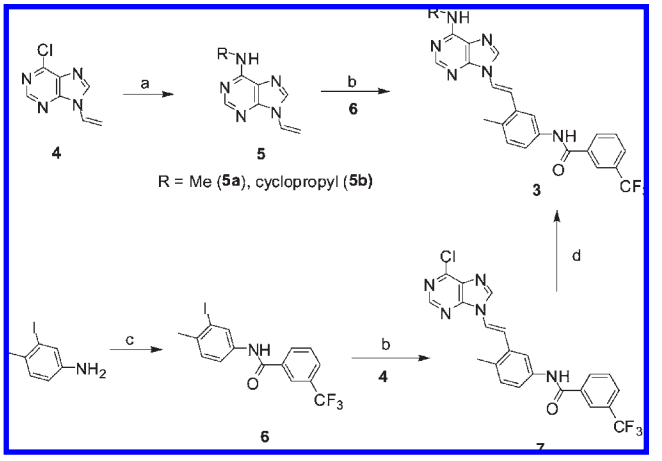

[a] Reagents and conditions: (a) RNH_2, THF, rt, 5 h; (b) 2.5 mol % $Pd(OAc)_2$, 5 mol % P(*o*-tol)$_3$, 120 mol % (*i*-Pr)$_2$NEt, DMF, 100 °C, 15 h; (c) 3-$CF_3C_6H_4CO_2H$, EDCI, HOBt, THF, rt, overnight; (d) 2 equiv $ArNH_2$, 10 mol % $Pd_2(dba)_3$, 15 mol % PhP(c-hexyl)$_2$, 1.5 equiv K_3PO_4, μW, 150 °C, 5 or 10 min.

Inhibitors **3c**, **3d**, **3e**, and **3f** were synthesized in the reverse order by first introducing the N^9-arenethenyl moiety onto the purine template followed by installation of the arylamino group at C-6. Thus, Heck reaction of **4** with **6** generated a common intermediate **7**, which underwent palladium-catalyzed *N*-arylation with various aryl amines to furnish the targeted compounds.

As depicted in Scheme 2, the reverse amides **9** and the urea analogue **11** were prepared from a similar Heck coupling of **5b** with iodobenzamides **8** and *N*,*N*′-diarylurea **10**, respectively. The precursors **8** were assembled by coupling 3-iodo-4-methylbenzoyl chloride with a variety of aryl amines and **10** was made from the addition of 3-iodo-4-methylaniline to 3-(trifluoromethyl)phenyl isocyanate.

Scheme 3 illustrates the preparation of inhibitors that bear further substitution on C-3″ of the B ring. For the synthesis of inhibitors **14**, the imidazole rings were coupled via copper-catalyzed *N*-arylations with 3-bromo-5-(trifluoromethyl)aniline in the presence of a bidentate ligand.[29] For the preparation of **17**, morpholine and 4-methylpiperazine were also introduced in the first step of the reaction sequence but via straightforward S_NAr displacement. It is noteworthy that

Table 1. In Vitro Assay Results of Inhibitors **2** and **3** (IC_{50} in nM)

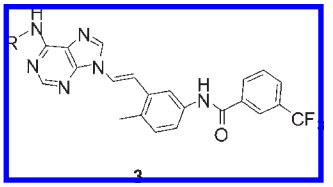

Cmpd.	R	Src kinase	Abl kinase	K562	WT Abl (Ba/F3)	Parental (Ba/F3)
2		300 (n = 1)	96 (n = 1)	n/a	>1000 (n = 1)	9678 (n = 2)
3a	Me	52 (n = 1)	25 (n = 1)	67 (n = 2)	47 (n = 3)	>10000 (n = 1)
3b		91 (n = 1)	74 (n = 1)	95 (n = 2)	57 (n = 3)	7857 (n = 1)
3c		201 (n = 2)	243 (n = 2)	181 (n = 2)	144 (n = 3)	6258 (n = 2)
3d		9.3 (n = 1)	26 (n = 1)	2.7 (n = 1)	n/a	>10000 (n = 1)
3e		4.7 (n = 2)	9.9 (n = 2)	3.7 (n = 3)	2.1 (n = 3)	635 (n = 2)
3f		26 (n = 1)	40 (n = 1)	62 (n = 3)	46 (n = 2)	2074 (n = 1)
3g		3.8 (n = 3)	5.7 (n = 3)	0.95 (n = 2)	2.5 (n = 5)	7597 (n = 3)
3h		159 (n = 1)	157 (n = 1)	n/a	n/a	n/a

Scheme 2. Preparation of Reverse Amides **9** and Urea **11**[a]

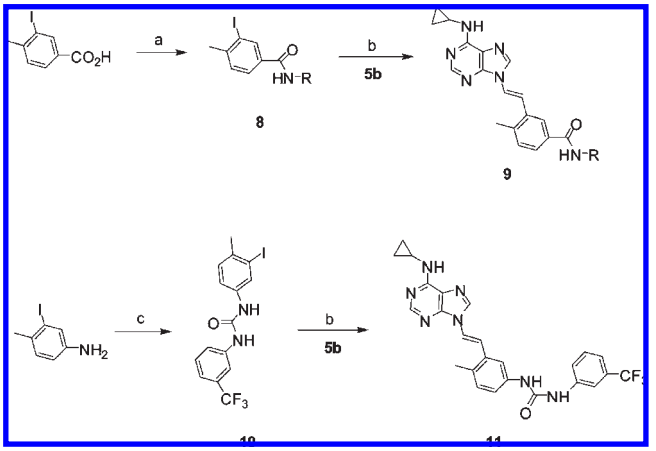

[a] Reagents and conditions: (a) (i) $SOCl_2$, reflux, 1 h, (ii) $ArNH_2$, $(i\text{-Pr})_2NEt$, cat. DMAP, THF, rt, 2 h; (b) 2.5 mol % $Pd(OAc)_2$, 5 mol % P(*o*-tol)$_3$, 120 mol % $(i\text{-Pr})_2NEt$, DMF, 100 °C, 15 h; (c) 3-$CF_3C_6H_4NCO$, CH_2Cl_2, rt, 4 h.

protection of the free amino group was unnecessary under both conditions. However, an excess of the nucleophiles was required to drive the S_NAr reaction to completion. Subsequent amide bond formation and Heck coupling furnished **14** and **17**.

Structure−Activity Relationship (SAR)

In vitro biological evaluation of the inhibitors included measuring their kinase inhibitory activity against both Src and Abl and their cellular activity associated with Bcr-Abl inhibition using both K562 (a human derived CML cell line expressing wild-type (WT) Bcr-Abl) and Ba/F3 cells transfected with wild-type Bcr-Abl. In general, potency in both cellular assays was comparable and consistent with SAR trends observed from the enzymatic assays. Inhibition of parental, nontransfected Ba/F3 cells was used as a control. Additionally, pharmacokinetic properties for active compounds were evaluated in rats to help guide series selection.

The prototype inhibitor **3a** demonstrated kinase IC_{50}s of 52 and 25 nM against Src and Abl, respectively, which validated our initial inhibitor design and original docking model. Moreover, when **3a** was tested in cells, it was remarkably potent against both cell lines without any effect on the parental control at concentrations up to 10 μM (Table 1). Reduction of **3a** to **2** resulted in decreased kinase and cellular activity, suggesting the more rigid double bond may introduce bias toward the preferred binding conformation. Interaction of the olefinic proton with the threonine gatekeeper residue via a pseudo hydrogen bond, as mentioned in our inhibitor design, could also have contributed to the enhanced potency of **3a**. Preliminary pharmacokinetic assessment of compound **3a** suggested it was cleared rapidly after being dosed orally in rats (vide infra). Previously, we have disclosed that the enamine-like N^9-(phenethenyl) moiety in the context of DFG-in targeted dual Src/Abl inhibitors is stable in vivo. For example, AP24149 (Figure 4, compound **10a** from reference 22) demonstrated oral bioavailability of approximately 20% in rats. Therefore, we speculated that the methylamino group at purine C-6 might be responsible for the poor oral bioavailability because the *N*-phenyl 3-trifluoromethyl-benzamide moiety has been highlighted in other orally bioavailable DFG-out targeted inhibitors.[23] To test this hypothesis, we substituted the methyl group with a cyclopropyl ring (**3b**), which is metabolically more stable and therefore less susceptible to rapid *N*-dealkylation. The preference for a cyclopropyl group was also partially due to the small change in molecular weight relative to **3a**. Gratifyingly, compound **3b** displayed satisfactory pharmacokinetics with high exposure and good oral bioavailability (F = 40%, Table 5) while maintaining target kinase potency and cellular activity.

Scheme 3. Preparation of Analogues **14** and **17** Bearing Additional B Ring Substitutions[a]

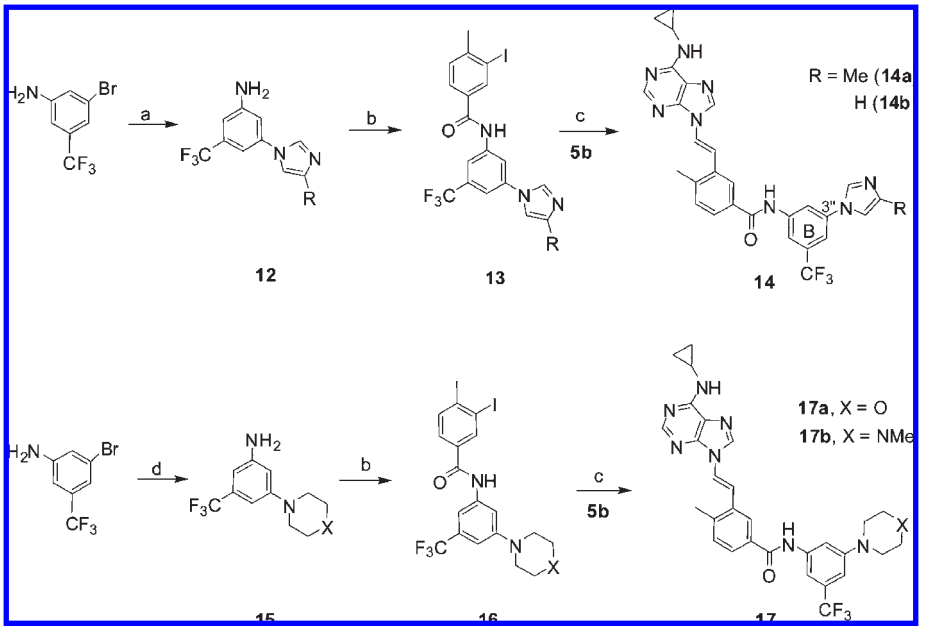

[a] Reagents and conditions: (a) imidazole or 4-methylimidazole, 15 mol % 8-hydroxyquinoline, 15 mol % CuI, 110 mol % K_2CO_3, DMSO, 120 °C, 15 h; (b) 3-iodo-4-methylbenzoyl chloride, $(i\text{-Pr})_2$NEt, THF, rt, 2 h; (c) 2.5 mol % $Pd(OAc)_2$, 5 mol % P(*o*-tol)$_3$, 120 mol % $(i\text{-Pr})_2$NEt, DMF, 100 °C, 15 h; (d) 4 equiv morpholine or 4-methylpiperazine, 2 equiv CsOH·H_2O, DMSO, 120 °C, 4 h.

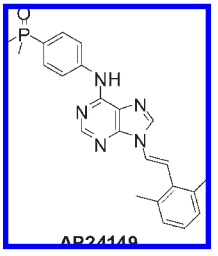

Figure 4. Orally bioavailable "DFG-in" N^9-(arenethenyl)purine.[22]

Encouraged by these data demonstrating that larger, lipophilic molecules like **3b** can be orally bioavailable, we focused on improving both the kinase and cellular potency through further SAR exploration at C-6 on the purine template. As shown in Table 1, several arylamines increased kinase activity while an alkyl derivative (**3h**) demonstrated reduced potency. This suggested the aryl rings might be engaged in hydrophobic or π stacking interactions with residues lining the hinge region. An exception was pyridine-2-ylamine (**3c**), which reduced kinase potency by about 50%. A tentative explanation for this observation is that the lone pair electrons on the 2-pyridyl N and those from N-1 on the purine template are repulsed, disrupting the coplanarity that contributes to optimal binding. In the case of the 3-pyridyl (**3d**) or 4-pyridyl (**3e**) derivatives, such electron repulsions do not exist. Instead, a nonclassical hydrogen bond between N-1 on purine template and the C-2′ aromatic proton on the pyridine ring might help stabilize the preferred coplanar conformation and hence, increase the kinase activity of **3d** and **3e**.[30] It is noteworthy that both compounds show dramatic increases in cellular potency with IC_{50}s for inhibition of K562 cells in the single digit nM range. Introduction of a (4-dimethylphosphinoyl)-phenyl moiety, one of the key molecular recognition elements responsible for the excellent potency observed with **1**, greatly improved potency in this series as well. Compound **3g** potently inhibited Src and Abl with IC_{50}s of 3.8 and 5.7 nM, respectively, and inhibited the proliferation of both cell lines in the single digit nM range. Additionally, this compound demonstrated excellent selectivity relative to the control cell line. Unfortunately, despite their increased kinase and cellular potencies, inhibitors **3d**, **3e**, and **3g** failed to demonstrate satisfactory preliminary pharmacokinetics. Therefore, in further optimization, we focused on inhibitors bearing a cyclopropylamine at C-6 of purine template.

Next, we briefly explored the reversed amide (**9**) and ureido (**11**) linkages connecting both pendent aryl rings at N-9 on the purine template (Table 2). Both linkers modeled well and were predicted to form the requisite hydrogen bonds to the protein. Compound **9a**, which bears the same amide linkage as nilotinib, was found to be slightly more potent than **3b** that has a "imatinib-like" amide. Urea **11** displayed a marked decrease in potency against Src kinase but almost no change relative to Abl, which may reflect different activation loop conformations adopted by the inactive forms of both Src and Abl. Nevertheless, molecule **11** demonstrated poor cellular activity in K562 cells (IC_{50} > 1 μM) and was not pursued further.

With the amide linkage optimized, we explored SAR on the pendent B-ring in the DFG binding pocket. Simple halogenation at either the ortho or the para position (**9b** and **9c**) slightly reduced potency relative to **9a**. Next we explored the possibility of replacing the trifluoromethyl group with reduced molecular weight and/or smaller hydrophobic substituents. *tert*-Butyl group substitution (**9d**) retained potency relative to **9a**, while the isopropyl analogue (**9e**) exhibited a 3−6 fold decrease depending upon the enzyme. This could be rationalized by the larger volume of the *tert*-butyl group relative to isopropyl and the consequential increased van der Waals contact in the well-defined hydrophobic pocket. Nevertheless, the *tert*-butyl derivative (**9d**) had a higher cLogP[31] relative to **9a** (6.76 vs 6.24, respectively), which we viewed as undesirable. To counterbalance this, we explored incorporating heteroatoms through several commercially available five-membered heteroaryls bearing *tert*-butyl substituents.

Table 2. In Vitro Assay Results of Inhibitors **9** and **11** (IC_{50} in nM)

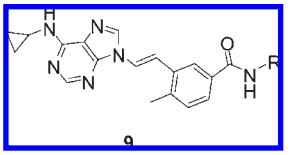

9

Cmpd.	R	Src kinase	Abl kinase	K562	WT Abl (Ba/F3)	Parental (Ba/F3)
9a	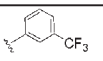	11 (n = 2)	23 (n = 2)	17 (n = 3)	10 (n = 2)	4353 (n = 1)
11		517 (n = 1)	62 (n = 1)	>1000 (n = 1)		
9b	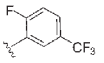	86 (n = 2)	236 (n = 2)	68 (n = 3)	57 (n = 3)	7665 (n = 1)
9c	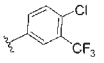	45 (n = 1)	37 (n = 1)	69 (n = 3)	48 (n = 2)	2409 (n =1)
9d	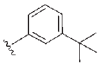	4.8 (n = 1)	59 (n = 1)	22 (n = 3)	16 (n = 2)	2554 (n =1)
9e	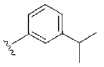	46 (n = 1)	60 (n = 1)	63 (n = 2)	60 (n = 3)	8318 (n = 2)
9f	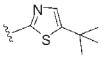	310 (n = 2)	267 (n = 2)	292 (n = 3)	195 (n = 3)	7120 (n = 3)
9g	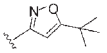	6.6 (n = 1)	23 (n = 1)	15 (n = 3)	12 (n = 3)	>10000 (n = 2)
9h	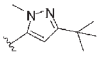	46 (n = 1)	146 (n = 1)	35 (n = 3)	31 (n = 2)	9031 (n =1)
9i	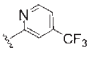	7.0 (n = 3)	20 (n = 3)	6.1 (n = 6)	4.8 (n = 3)	4894 (n = 4)

Gratifyingly, isoxazole analogue **9g** (cLogP = 5.29) was found to retain potency relative to **9a** against both target kinases. Despite this, both **9d** and **9g** exhibited less desirable rat pharmacokinetics (vide infra) relative to **9a** and this series was abandoned. Further work to reduce the lipophilicity of **9a** through heteroatom incorporation ultimately led to the discovery of **9i** (cLogP = 5.32), which not only maintained enzymatic and cell-based potency but also demonstrated increased exposure and was essentially 100% orally bioavailable.

The then-recent structural disclosure of nilotinib and its increased potency relative to imatinib prompted us to make several compounds based on this modified B ring (**14a**, **14b**) and, more generally, analogues in which alternative heterocyclic rings were installed at the C-3″ position (**17**) (Scheme 3 and Table 3). Inhibitors **14a** and **14b** retained Src and Abl potency relative to **9i**, while **17** displayed a slight decrease in potency, but overall, the impact of substitutions meta to the trifluoromethyl appeared to be minor.

Understanding Dual Src/Abl Activities

Many inhibitors (e.g., dasatinib,[12] bosutinib,[13a] and AZD0530;[13b] Figure 5), initially designed and synthesized for Src inhibition, were subsequently found to possess potent Abl inhibitory activity as well. This is not unexpected because of the high sequence homology between Src and Abl and their similar active DFG-in conformations. However, DFG-out Abl inhibitors do not necessarily possess potent Src inhibitory activity. It has been reported that neither imatinib nor nilotinib inhibits Src. The structural basis for Src inactivity of these potent DFG-out Abl binders is still not fully understood.[32] It is generally believed that Abl can easily adopt a DFG-out conformation, whereas Src appears to pay a high intrinsic energetic penalty to adopt such a binding mode, which makes it challenging to design a potent DFG-out inhibitor against both Abl and Src.[33] To better understand why our DFG-out Abl inhibitors also possess strong affinity for Src, we docked **9i** into the DFG-out conformation of Src kinase. Because of the lack of a DFG-out Src/ligand cocrystal at the time and the very close resemblance of Lck and Src kinases, we built the DFG-out Src model based on a published DFG-out structure of Lck (PDB: 2og8).[34] As shown in this model (Figure 6), **9i** makes two H-bonds with the Src hinge region through purine N-7 and the cyclopropyl amine. Two additional H-bonds are formed from the amide group of **9i** to the DFG backbone and Glu310 of α helix C, respectively. Notice that the H-bonding pattern in Src is essentially identical to that predicted in the Abl model. Also, as in the Abl model, the methylphenyl group of **9i** binds to the selective hydrophobic pocket located behind the gatekeeper residue, while the (trifluoromethyl) pyridyl group binds to a hydrophobic pocket, which is typically occupied by Phe405 of Src in the DFG-in conformation. The similarity in H-bonding and van der Waals (vdw) interactions of **9i** with Src and Abl observed in these models could explain the dual activities of **9i** and other related inhibitors in this chemical series against Src and Abl.

Table 3. In Vitro Assay Results of Inhibitors **14** and **17** (IC_{50} in nM)

compd	Src kinase	Abl kinase	K562	WT Abl (Ba/F3)	parental (Ba/F3)
14a	7.6 (n = 8)	25 (n = 8)	4.3 (n = 7)	7.3 (n = 6)	6455 (n = 6)
14b	8.0 (n = 1)	13 (n = 1)	5.4 (n = 3)	4.2 (n = 3)	7120 (n = 2)
17a	33 (n = 1)	72 (n = 1)	17 (n = 3)	10 (n = 3)	2525 (n = 1)
17b	41 (n = 1)	24 (n = 1)	14 (n = 3)	11 (n = 3)	543 (n = 1)

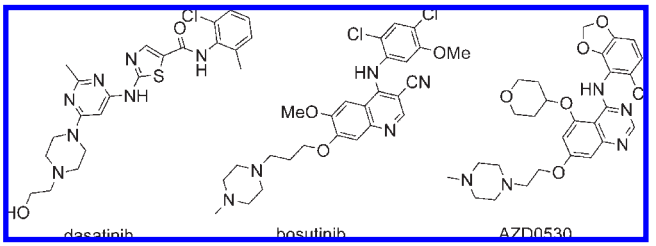

Figure 5. Representative dual Src/Abl kinase inhibitors targeting the "DFG-in" conformations.

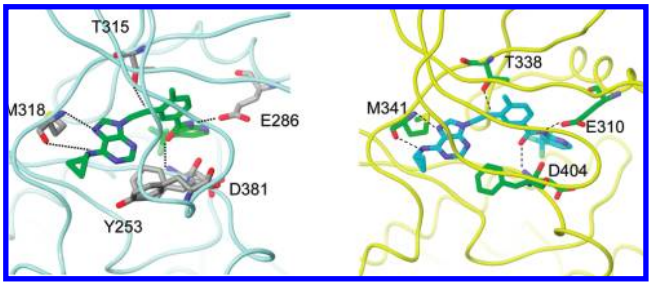

Figure 6. Model of compound **9i** bound to Abl (left) and Src (right).

Although the overall binding modes are similar, structural differences in loop conformations and ligand interactions are present in the docking models of Abl and Src. The largest difference resides in the conformation of the Gly-rich loops. The Gly-rich loop in Abl appears to be more flexible than that in Src based on a number of reported crystal structures of Abl and Src;[33,34] this loop is collapsed around bound inhibitors in Abl and makes numerous contacts with them. In contrast, the Gly-rich loop in Src adopts an extended conformation and makes minimal contacts with the inhibitor, as seen in our model and other reported crystal structures of Src (PDB: 3el7, 3el8) and its homologue Lck.[33,34] The loop conformational variation is contributed by the difference in amino acid sequence of the Gly-rich loops, especially Phe 278 in Src and Tyr253 in Abl, as well as their neighboring residues. The additional interactions of the Gly-rich loop with inhibitors make this class of compounds less sensitive to chemical modifications in terms of binding affinity to Abl. One modification introduced to **9i** was the removal of the C-6 substituent, leading to the loss of the hydrogen bond donor to the hinge region, as exemplified by inhibitors **18a** and **18b** (Table 4). Comparative kinase inhibition data indicated that the modification had little effect on Abl potency but had a much larger impact on Src. In fact, as shown in Table 4, compound **18a** is 10-fold less potent than **14a**, while **18b** is 45 times less potent than **9i** in the Src kinase assay. Interestingly, the same hydrogen bond donor to the hinge region is also absent in imatinib and nilotinib, both of which have minimal activities against Src. Taken together, structural differences in Abl and Src do exist despite the overall similarity and these differences can lead to Abl or Src specific inhibitors targeting the DFG-out conformation. Particularly, in this 9-(arenethenyl)purine series of DFG-out inhibitors, it appears that the Src inhibitors are more dependent on the formation of two H-bonds to the hinge region to gain potency, whereas Abl inhibitors bearing a single H-bond acceptor to the hinge region can achieve the same degree of potency due to additional interactions with the Gly-rich loop.

Pharmacokinetics of Selected Compounds

During this program, potent inhibitors were continually evaluated for their pharmacokinetic (PK) properties immediately following the assessment of their in vitro activity (Table 5). We observed that the introduction of certain functionalities consistently resulted in poor pharmacokinetics. Such examples included heteroarylamines (**3d**, **3e**) and certain 4-substituted anilines (e.g., **3g**) at C-6 on the purine core. To the contrary, compounds incorporating a 6-cyclopropylamine at the same position usually displayed favorable PK profiles (**3b**, **9g**, **9i**, **14a**). Both **9i** and **14a** exhibited low rates of clearance and high oral exposure. As a prerequisite to evaluating both compounds in in vivo efficacy models, PK parameters for both were determined orally in mice at three different doses; excellent dose proportionality was observed for both compounds (data not shown).

In Vivo Efficacy

The excellent in vitro kinase and cellular potency coupled with desirable pharmacokinetics of inhibitor **9i** prompted us to evaluate its antitumor activity in vivo in two well-established mouse efficacy models. In the first model, Ba/F3 cells expressing wild-type Bcr-Abl were injected into the tail vein of SCID mice. After 3 days, the animals were dosed orally with **9i** (Figure 7) at 10 mg/kg once daily for 19 consecutive days. In the control group, median survival was approximately 20 days with noted splenomegaly at autopsy. In the **9i** treated animals, median survival was approximately 35 days, representing a 75% increase in overall survival relative to control. For comparison, similar efficacy was observed in nilotinib treated animals at an oral dose of 75 mg/kg/day. In the second efficacy model, to evaluate Src inhibitory activity, subcutaneous tumors were established with NIH 3T3 cells transfected with constitutively activated Src Y527F. Daily oral administration of **9i** elicited dose-dependent tumor shrinkage with complete tumor growth inhibition observed at the highest dose (Figure 8).

Compound 14 Inhibits Bcr-Abl Mutant T315I

To determine whether any of our compounds possessed activity against the refractory T315I mutant,[6] we screened several compounds in an Abl-T315I kinase assay and ultimately in Ba/F3 cells transfected with Bcr-Abl T315I. Interestingly, two inhibitors bearing imidazole appendages on the B ring, **14a** and **14b**, demonstrated modest kinase inhibition and inhibited the proliferation of such Ba/F3 cells with IC_{50}s between 300 and 400 nM (Table 6). Moreover, inhibition of

Table 4. Impact of Additional H-Bond with Hinge on Potency (IC_{50} in nM)

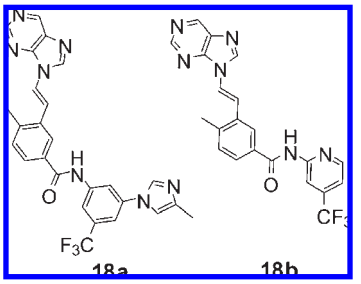

compd	Src kinase	Abl kinase	WT Abl (Ba/F3)
14a	8	25	9
18a	84	48	7
9i	7	20	6
18b	307	38	5

Table 5. Mean Pharmacokinetic Parameters Following Intravenous (iv) or Oral Dosing (po) in CD Rats or Mice [a]

	iv			po			
compd	CL (L/h/ kg)	V_d (L/kg)	$t_{1/2}$ (h)	$AUC_{0-24\ h}$ (ng·h/mL)	C_{max} (ng/mL)	t_{max} (h)	F (%)
3a	0.38	1.60	2.95	N/C[e]	N/C	N/C	N/C
3b	0.19[b]	1.08	4.0	32151[c]	2613	1.0	40
3d	0.49[b]	1.70	2.4	3311[c]	387	2.0	11
3e	0.96[b]	9.01	6.7	N/C	483	6.0	N/C
3g	0.79[b]	3.54	3.1	146[c]	63	1.0	0.8
9d	1.79[b]	5.31	2.1	297[c]	100	1.0	3.5
9g	0.90[b]	4.87	3.7	7540[c]	1040	1.0	45
9i	0.04[b]	0.34	5.7	428459[c]	23525	2.0	116
14a	0.06[b]	0.78	8.3	17249[c]	1753	2.0	7
9i				21195[d]	3097	2.0	
14a				6927[d]	1020	1.0	

[a] $n = 3$ animals per study. [b] Dosed iv in rats at 5 mg/kg as a solution in 50% DMA, 45% PEG-400, and 5% Tween-80. [c] Dosed po in rats at 15 mg/kg as a solution 15% DMA, 15% TPGS, 5% Tween-80, 25% PEG-400, and 40% water. [d] Dosed po in mice at 10 mg/kg as a solution in 15% DMA, 15% TPGS, 5% Tween-80, 25% PEG-400, and 40% water. [e] N/C = not calculated.

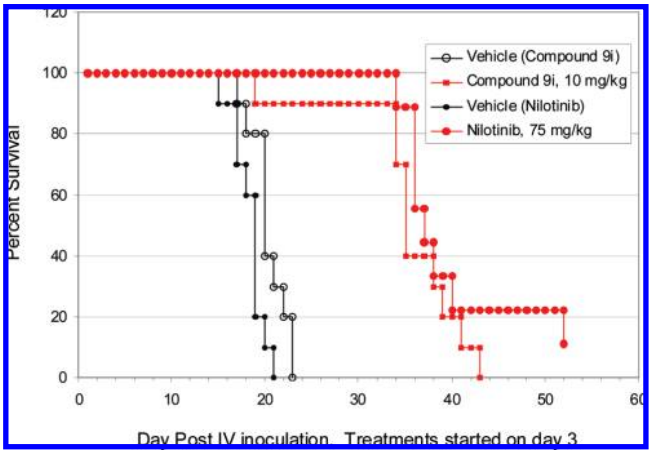

Figure 7. In vivo efficacy of **9i** in a Ba/F3 WT Bcr-Abl survival model.

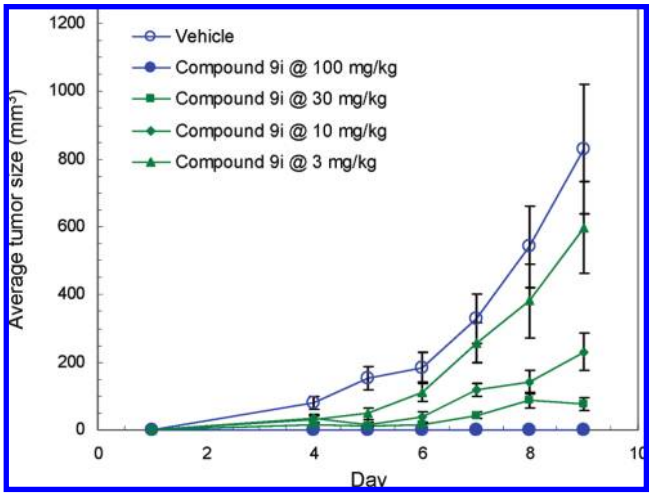

Figure 8. In vivo efficacy of **9i** in a Src Y527F mouse tumor model.

cell proliferation by **14a** directly correlated with decreased cellular phosphorylation of pBcr-Abl (data not shown, see ref 35) and the IC_{50} for inhibition of the nontransfected parental Ba/F3 control was greater than 6 μM. Inhibitors bearing other ring systems (**17**) or without substitution at the C-3″ position (**9i**) were either less effective or completely inactive against this mutation. Previously, we observed that compounds bearing these substitutions gave rise to only minor changes in potency against wild type Abl. The model of **14a** docked into T315I Abl kinase demonstrates that the 4-methylimidazole group fills a shallow pocket formed by Glu228, Glu282, Val289, Asp381, and Phe359 (Figure 9). This additional interaction with the protein appears to contribute

Table 6. Inhibition of Bcr-Abl Mutant T315I (IC_{50} in nM)

	14a	14b	17a	17b	9i
T315I kinase	478	542	> 5000	1818	14412
T315I (Ba/F3)	422	298	nd	nd	2746

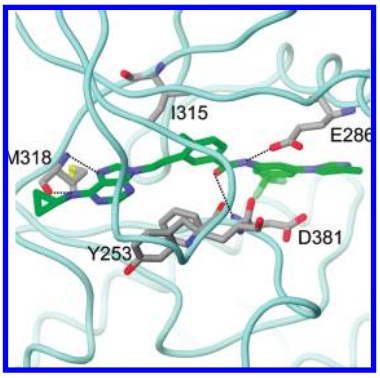

Figure 9. Model of compound **14a** bound to Abl T315I.

significantly to its activity against T315I. It is noteworthy that inhibitor **14a** shares an identical structural fragment with nilotinib but that the latter is completely ineffective against Abl T315I. When nilotinib is docked into the model of Abl kinase with the T315I mutation, there is an obvious steric clash between the amino group on the pyrimidine ring and the larger isoleucine residue. Such a clash is not observed between the less sterically demanding double bond linkage in **14a**, which may explain its increased activity against this important clinical mutation.

To further characterize the activity of **14a**, we also determined the antiproliferation activity against a broader panel of Ba/F3 cells expressing clinically relevant Bcr-Abl mutants: L248R, G250E, Q252H, Y253H, and E255K. Relative to T315I-expressing cells, these cell lines were more potently inhibited with IC_{50}s of 64, 63, 42, 44, and 24 nM, respectively, which is comparable or superior to the potency of nilotinib against the same mutations.[16a]

Conclusion

Through our program of structure guided drug design, we have identified a novel series of purine-based compounds that potently inhibit Src and Abl by specifically targeting the inactive conformation of both proteins. Extensive SAR revealed structural features contributing to high potency. Several key ligand−protein interactions responsible for potency against both kinases include a hydrogen bond between the hinge region and N-7 on the purine core, hydrogen bonds between the amide group and the Glu residue in the αC-helix and Asp residue in the DFG motif, respectively, and hydrophobic interaction between the trifluoromethylphenyl and the proteins. The NH at C-6 on the purine template was identified as critical for achieving high potency against Src through a well-defined hydrogen bond with a hinge residue. Compounds bearing cyclopropylamine at C-6 on the purine core were found to display highly desirable pharmacokinetics in general. Once-daily oral administration of inhibitor **9i** (AP24226)[36] at 10 mg/kg significantly prolonged the survival of mice injected intravenously with wild type Bcr-Abl expressing Ba/F3 cells, with potency comparable to nilotinib when dosed at 75 mg/kg. Furthermore, **9i** also elicited dose-dependent tumor shrinkage in a Src Y527F mouse tumor model at oral doses ranging from 10 to 100 mg/kg. Inhibitor **14a** (AP24163),[36] an alternative member of this novel series, not only potently inhibits both Src and Abl but also displays clear cellular potency against a number of clinically identified Bcr-Abl mutants including the highly refractory T315I mutation. Its modest cellular potency (IC_{50} = 420 nM) against T315I is encouraging given the insensitivity of this mutant to all currently marketed first- and second-generation Bcr-Abl inhibitors.

Experimental Section

Chemistry. All reagents and solvents were used as received. ^{1}H NMR (300.1 MHz), ^{19}F NMR (282.4 MHz), and ^{31}P NMR (121.5 MHz) spectra were recorded on a Bruker ARX300 spectrometer, using TMS as internal standard and $CFCl_3$ or 85% H_3PO_4 as external standard, respectively. MS spectra were recorded on a Waters Micromass ZQ spectrometer. Elemental analyses were performed by Robertson Microlit Laboratories in Madison, NJ. HPLC was performed on an Agilent 1100 HPLC system. The purity of all SAR compounds was determined to be ≥95% by reverse phase HPLC (C-18 column, MeCN/H_2O with 0.1% CF_3CO_2H as the mobile phase), and certain compounds were further checked for their purity via combustion analysis.

General Procedure for the Preparation of 6-(Alkylamino)-9-vinylpurines 5; *N*-methyl-9-vinyl-9*H*-purin-6-amine (5a), Method A. 6-Chloro-9-vinylpurine[28](0.54 g, 3 mmol) was added to the solution of methylamine (7.5 mL, 15 mmol, 2.0 M in THF) in THF (5 mL), and the mixture was stirred for 5 h at rt. Water was added to dissolve the white precipitate (methylamine hydrochloride). The aqueous layer was extracted with ethyl acetate, and the combined organic layers were dried over sodium sulfate, concentrated on a rotavap, and then subjected to silica gel column chromatography (5% methanol/methylene chloride), yielding the desired product as white solid in 75% yield. ^{1}H NMR (CD_3OD): δ 3.11 (s, 3H), 5.18 (dd, J = 9.2, 1.3 Hz, 1H), 5.97 (dd, J = 16.0, 1.3 Hz, 1H), 7.28 (dd, J = 16.0, 9.2 Hz, 1H), 8.28 (s, 1H), 8.32 (s, 1H).

***N*-Cyclopropyl-9-vinyl-9*H*-purin-6-amine (5b).** Method A; yield: 92%. ^{1}H NMR ($CDCl_3$): δ 0.60 (m, 2H), 0.87 (m, 2H), 3.00 (m, 1H), 5.08 (dd, J = 9.1, 1.4 Hz, 1H), 5.80 (dd, J = 16.0, 1.4 Hz, 1H), 6.39 (br, 1H), 7.20 (dd, J = 16.0, 9.1 Hz, 1H), 7.94 (s, 1H), 8.45 (s, 1H).

***N*-(4-(Dimethylphosphoryl)phenyl)-9-vinyl-9*H*-purin-6-amine (5g).** A mixture of 6-chloro-9-vinylpurine (0.18 g, 1 mmol), 4-dimethylphosphinylaniline (0.17 g, 1 mmol), and pyridine hydrochloride (0.11 g, 1 mmol) was dissolved in 2-ethoxyethanol (2 mL). The resulting solution was heated at 160 °C for 10 min under microwave irradiation. The mixture was concentrated to dryness on a rotavap. EtOAc and aq $NaHCO_3$ were added. The aqueous layer was extracted with ethyl acetate, and the combined organic layers were dried over sodium sulfate, concentrated on a rotavap, and then subjected to silica gel column chromatography (eluent: 10% methanol/methylene chloride), yielding the desired product in 56% yield. ^{1}H NMR (CD_3OD): δ 1.70 (d, J = 13.2 Hz, 3H), 1.81 (d, J = 13.3 Hz, 3H), 5.23 (d, J = 9.2 Hz, 1H), 6.07 (d, J = 16.0 Hz, 1H), 7.34 (dd, J = 16.0, 9.1 Hz, 1H), 7.33 (m, 2H), 7.79 (m, 2H), 8.46 (s, 1H), 8.50 (s, 1H).

***N*-(3-(*N*′,*N*′-Dimethylamino)propyl)-9-vinyl-9*H*-purin-6-amine (5h).** Method A; yield: 95%. ^{1}H NMR ($CDCl_3$): δ 2.00 (m, 2H), 2.44 (s, 6H), 2.67 (m, 2H), 3.80 (m, 2H), 5.15 (dd, J = 9.1, 1.4 Hz, 1H), 5.85 (dd, J = 16.0, 1.4 Hz, 1H), 6.63 (br, 1H), 7.23 (dd, J = 16.0, 9.1 Hz, 1H), 7.97 (s, 1H), 8.41 (s, 1H).

***N*-(3-Iodo-4-methylphenyl)-3-(trifluoromethyl)benzamide (6).** A solution of 3-iodo-4-methylaniline (1.22 g, 5.25 mmol), 3-(trifluoromethyl)benzoic acid (0.95 g, 5 mmol), HOBt (0.68 g, 5 mmol), and EDCI (1.05 g, 5.5 mmol) in THF (20 mL) was stirred overnight at rt. Water was added, and the aqueous layer

was extracted with dichloromethane. The combined organic layers were dried over sodium sulfate, concentrated on a rotavap, and then subjected to silica gel column chromatography (3:1 hexane/ethyl acetate), yielding the desired product as white solid in 83% yield. ^{1}H NMR (CD_3OD): δ 2.40 (s, 3H), 7.27 (d, J = 8.3 Hz, 1H), 7.62 (dd, J = 8.3, 2.2 Hz, 1H), 7.71 (dd, J = 7.8, 7.8 Hz, 1H), 7.87 (d, J = 7.9 Hz, 1H), 8.18 (d, J = 7.9 Hz, 1H), 8.25 (d, J = 7.9 Hz, 1H), 8.26 (dd, J = 7.9, 2.1 Hz, 1H).

General Procedure for the Heck Reaction of 9-Vinylpurines and Aryl Iodides; (*E*)-*N*-(4-Methyl-3-(2-(6-(methylamino)-9*H*-purin-9-yl)vinyl)phenyl)-3-(trifluoromethyl)-benzamide (3a), Method B. A solution of 9-vinylpurine **5a** (1 mmol), aryl iodide **6** (1.1 mmol), $Pd(OAc)_2$ (11.2 mg, 0.05 mmol), and P(*o*-tol)$_3$ (30.4 mg, 0.1 mmol) in DMF (3 mL) was degassed with bubbling N_2 for 10 min. (*i*-Pr)$_2$NEt (0.52 mL, 3 mmol) was added under N_2, The resulting solution was stirred at 110 °C for 15 h. Water was added, and the aqueous layer was extracted with EtOAc. The combined organic layers were dried over Na_2SO_4, concentrated on a rotavap, and then subjected to silica gel column chromatography (5% MeOH/CH_2Cl_2), yielding the desired product as white powder in 82% yield; mp 201 °C. ^{1}H NMR ($CDCl_3$): δ 2.42 (d, J = 7.9 Hz, 3H), 3.24 (s, 3H), 5.87 (s, 1H), 7.20 (d, J = 8.2 Hz, 1H), 7.48 (d, J = 14.5 Hz, 1H), 7.52 (dd, J = 7.1, 2.0 Hz, 1H), 7.59 (d, J = 14.5 Hz, 1H), 7.65 (d, J = 7.8 Hz, 1H), 7.81 (d, J = 8.2 Hz, 1H), 7.84 (d, J = 1.9 Hz, 1H), 8.02 (s, 1H), 8.11 (d, J = 7.8 Hz, 1H), 8.18 (s, 2H), 8.48 (s, 1H). ^{19}F NMR ($CDCl_3$): δ −61.92. MS [M + H]$^+$ 453.3.

(*E*)-*N*-(4-Methyl-3-(2-(6-(cyclopropylamino)-9*H*-purin-9-yl)vinyl)-phenyl)-3-(trifluoromethyl)benzamide (3b). Method B: This compound was made from **5b** and **6** in 56% yield. ^{1}H NMR (DMSO-d_6): δ 0.67 (m, 2H), 0.77 (m, 2H), 2.42 (s, 3H), 3.24 (m, 1H), 7.37 (d, J = 8.4 Hz, 1H), 7.68 (dd, J = 8.1, 1.9 Hz, 1H), 7.73 (s, 1H), 7.81 (d, J = 7.2 Hz, 1H), 7.82 (d, J = 14.5 Hz, 1H), 8.00 (d, J = 7.1 Hz, 1H), 8.07 (d, J = 2.0 Hz, 2H), 8.30 − 8.38 (m, 3H), 8.74 (s, 1H), 10.47 (s, 1H). ^{19}F NMR ($CDCl_3$): δ −57.17. MS [M + H]$^+$ 479.1. Anal. calcd for ($C_{25}H_{21}F_3N_6O\cdot 0.07CH_2Cl_2$): C, H, N.

(*E*)-*N*-(3-(2-(6-(4-(Dimethylphosphoryl)phenylamino)-9*H*-purin-9-yl)-vinyl)-4-methylphenyl)-3-(trifluoromethyl)benzamide (3g). Method B: This compound was made from **5g** and **6** in 47% yield. ^{1}H NMR (DMSO-d_6): δ 1.65 (d, J = 13.2 Hz, 6H), 2.44 (s, 3H), 7.29 (d, J = 8.2 Hz, 1H), 7.69 (dd, J = 7.2, 1.9 Hz, 1H), 7.73−7.87 (m, 3H), 7.78 (d, J = 14.8 Hz, 1H), 7.90 (d, J = 14.7 Hz, 1H), 8.00 (d, J = 7.8 Hz, 1H), 8.11 (m, 1H), 8.14 (d, J = 2.0 Hz, 1H), 8.17 (d, J = 2.0 Hz, 1H), 8.32 (d, J = 8.2 Hz, 1H), 8.36 (s, 1H), 8.60 (s, 1H), 8.97 (s, 1H), 10.29 (s, 1H), 10.49 (s, 1H). ^{19}F NMR (DMSO-d_6): δ −57.17. ^{31}P NMR (DMSO-d_6): δ 36.77. MS [M + H]$^+$ 591.4. Anal. calcd for ($C_{30}H_{26}F_3N_6O_2P\cdot 0.25 CH_2Cl_2$): C, H, N.

(*E*)-*N*-(4-Methyl-3-(2-(6-(3-(*N*′,*N*′-dimethylamino)propylamino)-9*H*-purin-9-yl)vinyl)phenyl)-3-(trifluoromethyl)benzamide (3h). Method B: This compound was made from **5h** and **6** in 45% yield. ^{1}H NMR ($CDCl_3$): δ 1.74 (tt, J = 6.6, 6.6 Hz, 2H), 2.16 (s, 6H), 2.32 (s, 3H), 2.34 (t, J = 6.7 Hz, 2H), 3.64 (m, 2H), 6.75 (t, J = 5.3 Hz, 1H), 7.00 (d, J = 8.3 Hz, 1H), 7.21 (d, J = 17.5 Hz, 1H), 7.34 (d, J = 17.6 Hz, 1H), 7.39 (dd, J = 8.2, 2.1 Hz, 1H), 7.46 (d, J = 7.8 Hz, 1H), 7.59 − 7.65 (m, 2H), 7.85 (s, 1H), 7.94 (d, J = 2.9 Hz, 1H), 8.09 (s, 1H), 8.31 (s, 1H), 8.68 (s, 1H). ^{19}F NMR ($CDCl_3$): δ −63.45. MS [M + H]$^+$ 524.4. Anal. calcd for ($C_{27}H_{28}F_3N_7O$): C, H, N.

***N*-(4-Methyl-3-(2-(6-(methylamino)-9*H*-purin-9-yl)ethyl)phenyl)-3-(trifluoromethyl)-benzamide (2).** To a solution of **3a** (0.10 g) in MeOH was added a catalytic amount of 10% palladium on carbon. The resulting mixture was hydrogenated under 50 psi H_2 for 48 h, at which point HPLC indicated completion. The catalyst was removed by filtration, and the filtrate was concentrated on a rotavap and further dried under vacuum, giving the desired product in quantitative yield. ^{1}H NMR ($CDCl_3$): δ 2.13 (d, J = 7.3 Hz, 3H), 3.21 (t, J = 7.1 Hz, 2H), 3.30 (s, 3H), 4.47 (t, J = 7.1 Hz, 2H), 7.17 (d, J = 8.2 Hz, 1H), 7.37 (d, J = 7.5 Hz, 1H), 7.48 (s, 1H), 7.55 (s, 1H), 7.65 (dd, J = 7.8, 7.7 Hz, 1H), 7.81 (s, 1H), 7.85 (d, J = 7.5 Hz, 1H), 8.08 (d, J = 7.9 Hz, 1H), 8.13 (s, 1H), 8.33 (s, 1H). MS [M + H]$^+$ 455.3.

(*E*)-*N*-(3-(2-(6-Chloro-9*H*-purin-9-yl)vinyl)-4-methylphenyl)-3-(trifluoromethyl)-benzamide (7). Method B: 29% yield. ^{1}H NMR (DMSO-d_6): δ 2.42 (s, 3H), 7.28 (d, J = 8.3 Hz, 1H), 7.67 (dd, J = 8.2, 2.1 Hz, 1H), 7.77 (d, J = 14.7 Hz, 1H), 7.80 (dd, J = 7.9, 7.8 Hz, 1H), 7.92 (d, J = 14.7 Hz, 1H), 8.00 (d, J = 7.9 Hz, 1H), 8.12 (d, J = 2.0 Hz, 1H), 8.30 (d, J = 8.0 Hz, 1H), 8.34 (s, 1H), 8.92 (s, 1H), 9.24 (s, 1H), 10.49 (s, 1H). MS [M − H]$^+$ 455.6.

General Procedure for the Preparation of 3 from Pd-Catalyzed Amination of 7 with Arylamines; (*E*)-*N*-(4-Methyl-3-(2-(6-(pyridine-2-yl-amino)-9*H*-purin-9-yl)vinyl)phenyl)-3-(trifluoromethyl)-benzamide (3c), Method C. A mixture of compound **7** (46 mg, 0.1 mmol), 2-aminopyridine (22 mg, 0.2 mmol), dicyclohexylphenylphosphine (11 mg, 0.03 mmol), $Pd_2(dba)_3$ (18 mg, 0.02 mmol), and K_3PO_4 (32 mg, 0.15 mmol) was charged in a microwave reaction tube and then degassed via three cycles of vacuum−Ar refilling. Anhydrous DMF (1 mL) was added, and the resulting solution was heated under microwave at 150 °C for 5 min. After cooling to rt, the reaction mixture was filtered and subjected to a silica gel column chromatography (5−10% methanol/methylene chloride), giving the desired product as white solid in 36% yield. ^{1}H NMR ($CDCl_3$): δ 2.41 (s, 3H), 7.03 (dd, J = 6.1, 5.9 Hz, 1H), 7.19 (d, J = 6.8 Hz, 1H), 7.49 (s, 1H), 7.52 (d, J = 8.2 Hz, 1H), 7.61−7.69 (m, 2H), 7.76−7.83 (m, 2H), 7.89 (s, 1H), 8.13−8.19 (m, 4H), 8.34 (d, J = 3.7 Hz, 1H), 8.66 (s, 1H), 8.68 (m, 1H). ^{19}F NMR ($CDCl_3$): δ −63.49. MS [M]$^+$ 515.1.

(*E*)-*N*-(4-Methyl-3-(2-(6-(pyrid-3-yl-amino)-9*H*-purin-9-yl)vinyl)phenyl)-3-(trifluoromethyl)-benzamide (3d). Method C: purified by reverse phase prep-HPLC (MeCN/H_2O, 0.1% TFA) as TFA salt. ^{1}H NMR (DMSO-d_6): δ 2.43 (s, 3H), 7.28 (d, J = 8.3 Hz, 1H), 7.66−7.70 (m, 2H), 7.74 (s, 1H), 7.79 (s, 1H), 7.83 (d, J = 7.9 Hz, 1H), 7.87−7.94 (m, 1H), 8.00 (d, J = 8.0 Hz, 1H), 8.12 (d, J = 1.9 Hz, 1H), 8.30−8.35 (m, 2H), 8.42 (d, J = 5.0 Hz, 1H), 8.63 (s, 1H), 9.00 (s, 1H), 9.35 (d, J = 2.2 Hz, 1H), 10.49 (s, 1H), 10.61 (s, 1H). ^{19}F NMR ($CDCl_3$): δ −57.09, −70.31. MS [M]$^+$ 515.4.

(*E*)-*N*-(4-Methyl-3-(2-(6-(pyrid-4-yl-amino)-9*H*-purin-9-yl)vinyl)phenyl)-3-(trifluoromethyl)-benzamide (3e). Method C: purified by reverse phase prep-HPLC (MeCN/H_2O, 0.1% TFA) as TFA salt. ^{1}H NMR (DMSO-d_6): δ 2.44 (s, 3H), 7.30 (d, J = 8.2 Hz, 1H), 7.66 (d, J = 7.7 Hz, 1H), 7.77 − 7.84 (m, 2H), 7.94 (d, J = 14.8 Hz, 1H), 8.00 (d, J = 7.7 Hz, 1H), 8.16 (s, 1H), 8.31 (d, J = 8.2 Hz, 1H), 8.35 (s, 1H), 8.58 (d, J = 6.9 Hz, 2H), 8.70 (d, J = 6.9 Hz, 2H), 8.86 (s, 1H), 9.17 (s, 1H), 10.50 (s, 1H), 11.70 (s, 1H). ^{19}F NMR ($CDCl_3$): δ −57.09, −69.99. MS [M]$^+$ 515.6.

(*E*)-*N*-(4-Methyl-3-(2-(6-(pyrimid-4-yl-amino)-9*H*-purin-9-yl)-vinyl)-phenyl)-3-(trifluoromethyl)-benzamide (3f). Method C: purified by reverse phase prep-HPLC (MeCN/H_2O, 0.1% TFA) as TFA salt. ^{1}H NMR (DMSO-d_6): δ 2.27 (s, 3H), 7.25 (d, J = 8.3 Hz, 1H), 7.69 (dd, J = 7.9, 1.9 Hz, 1H), 7.70 (d, J = 15.0 Hz, 1H), 7.76 (d, J = 15.5 Hz, 1H), 7.78 (s, 1H), 7.82 (d, J = 7.8 Hz, 1H), 7.98 (d, J = 7.7 Hz, 1H), 8.05 (d, J = 1.9 Hz, 1H), 8.23 (d, J = 5.8 Hz, 1H), 8.32 (d, J = 8.1 Hz, 1H), 8.34 (d, J = 5.6 Hz, 1H), 8.36 (d, J = 6.2 Hz, 1H), 8.60 (s, 1H), 8.66 (s, 1H), 10.49 (s, 1H). ^{19}F NMR ($CDCl_3$): δ −57.16. MS [M]$^+$ 516.7. Anal. calcd for ($C_{26}H_{19}F_3N_8O\cdot 0.6CF_3CO_2H$): C, H, N.

General Procedure for the Preparation of 3-Iodo-4-methylbenzamides 8; 3-Iodo-4-methyl-*N*-(4-(trifluoromethyl)pyridin-2-yl) benzamide (8i), Method D. 3-Iodo-4-methylbenzoic acid (2.62 g, 10 mmol) was refluxed in $SOCl_2$ (10 mL) for 1 h. The volatile components were removed on a rotavap, and the residue was dissolved in benzene (10 mL), concentrated to dryness on a rotavap, and further dried under vacuum. The resulting acyl chloride was added to a solution of 2-amino-4-(trifluoromethyl) pyridine (1.65 g, 10.2 mmol), *N*,*N*-diisopropylethylamine (1.56 g, 12 mmol), and a catalytic amount of DMAP in THF (20 mL). After stirring at rt for 2 h, the reaction was quenched with water. EtOAc was added, and the layers were separated. The combined organic layers were concentrated to dryness, giving a mixture of desired product (major) and bis-acylated

byproduct; the latter is slightly less polar (TLC) but difficult to separate by column chromatography. The product mixture was then dissolved in THF (30 mL) and stirred with 4 N aq NaOH (30 mL) at 50 °C for 15 min. Extraction with EtOAc followed by concentration of combined organic layers gave the desired product, which was pure by NMR and used in next step without purification. Yield: 95%. ^{1}H NMR (DMSO-d_6): δ 2.45 (s, 3H), 7.48 (d, J = 8.1 Hz, 1H), 7.54 (dd, J = 5.1, 1.9 Hz, 1H), 7.97 (dd, J = 7.9, 1.8 Hz, 1H), 8.49 (d, J = 1.8 Hz, 1H), 8.51 (m, 1H), 8.68 (d, J = 5.1 Hz, 1H), 11.33 (s, 1H). MS $[M + H]^+$ 407.0.

***N*-(3-(*tert*-Butyl)phenyl)-3-iodo-4-methylbenzamide (8d).** Method D. ^{1}H NMR (DMSO-d_6): δ 1.29 (s, 9H), 2.45 (s, 3H), 7.14 (dtt, J = 7.9, 1.8, 1.0 Hz, 1H), 7.09 (dd, J = 7.9, 7.9 Hz, 1H), 7.48 (d, J = 8.1 Hz, 1H), 7.66 (dtt, J = 8.0, 1.9, 1.0 Hz, 1H), 7.75 (dd, J = 1.9, 1.8 Hz, 1H), 7.91 (dd, J = 7.9, 1.8 Hz, 1H), 8.41 (d, J = 1.8 Hz, 1H), 10.16 (s, 1H).

***N*-(3-(*iso*-Propyl)phenyl)-3-iodo-4-methylbenzamide (8e).** Method D. ^{1}H NMR (DMSO-d_6): δ 1.22 (d, J = 6.9 Hz, 6H), 2.44 (s, 3H), 2.88 (septet, J = 6.9 Hz, 1H), 6.99 (d, J = 7.7 Hz, 1H), 7.26 (dd, J = 7.8, 7.7 Hz, 1H), 7.48 (d, J = 8.0 Hz, 1H), 7.61 − 7.63 (m, 2H), 7.91 (dd, J = 7.9, 1.8 Hz, 1H), 8.41 (d, J = 1.8 Hz, 1H), 10.16 (s, 1H).

***N*-(5-(*tert*-Butyl)-1*H*-oxazo-3-yl)-3-iodo-4-methylbenzamide (8g).** Method D. ^{1}H NMR ($CDCl_3$): δ 1.39 (s, 9H), 2.52 (s, 3H), 6.84 (s, 1H), 7.37 (d, J = 7.9 Hz, 1H), 7.84 (dd, J = 7.9, 1.7 Hz, 1H), 8.40 (d, J = 1.7 Hz, 1H), 9.36 (s, 1H).

***N*-(1-Methyl-3-(*tert*-butyl)-1*H*-pyrazo-5-yl)-3-iodo-4-methylbenzamide (8h).** Method D. ^{1}H NMR (DMSO-d_6): δ 1.23 (s, 9H), 2.45 (s, 3H), 3.61 (s, 3H), 6.09 (s, 1H), 7.49 (d, J = 8.1 Hz, 1H), 7.89 (dd, J = 7.9, 1.7 Hz, 1H), 8.39 (d, J = 1.7 Hz, 1H), 10.24 (s, 1H).

(*E*)-3-(2-(6-(Cyclopropylamino)-9*H*-purin-9-yl)vinyl)-4-methyl-*N*-(3-(trifluoromethyl)phenyl)benzamide (9a). Method B. ^{1}H NMR ($CDCl_3$): δ 0.71 (m, 2H), 0.97 (m, 2H), 2.50 (s, 3H), 3.13 (m, 1H), 7.34 (d, J = 7.9 Hz, 1H), 7.41 (d, J = 8.0 Hz, 1H), 7.48 (d, J = 8.0 Hz, 1H), 7.55 (d, J = 16.0 Hz, 1H), 7.62 (s, 1H), 7.66 (s, 1H), 7.73 (dd, J = 7.9, 1.8 Hz, 1H), 7.93 (d, J = 8.2 Hz, 1H), 8.01 (s, 1H), 8.07 (m, 2H), 8.23 (s, 1H), 8.50 (s, 1H). Anal. calcd for ($C_{25}H_{21}F_3N_6O \cdot 0.02CH_2Cl_2$): C, H, N.

(*E*)-3-(2-(6-(Cyclopropylamino)-9*H*-purin-9-yl)vinyl)-4-methyl-*N*-(2-fluoro-5-(trifluoromethyl)phenyl)benzamide (9b). Method B; purified by reverse phase prep-HPLC (MeCN/H_2O, 0.1% TFA) as TFA salt. ^{1}H NMR (DMSO-d_6): δ 0.72 (m, 2H), 0.82 (m, 2H), 2.51 (s, 3H), 2.98 (m, 1H), 7.44 (d, J = 8.1 Hz, 1H), 7.58 (dd, J = 9.6, 9.2 Hz, 1H), 7.68 (m, 1H), 7.85 (dd, J = 7.9, 1.8 Hz, 1H), 7.90 (d, J = 10.0 Hz, 1H), 7.94 (d, J = 14.7 Hz, 1H), 7.85 (dd, J = 7.9, 1.8 Hz, 1H), 8.11 (dd, J = 6.7, 1.9 Hz, 1H), 8.29 (d, J = 1.5 Hz, 1H), 8.46 (s, 1H), 8.80 (s, 1H), 10.43 (s, 1H). MS $[M + H]^+$ 496.7. Anal. calcd for ($C_{25}H_{20}F_4N_6O \cdot 1.7CF_3CO_2H$): C, H, N.

(*E*)-3-(2-(6-(Cyclopropylamino)-9*H*-purin-9-yl)vinyl)-4-methyl-*N*-(4-chloro-3-(trifluoromethyl)phenyl)benzamide (9c). Method B; purified by reverse phase prep-HPLC (MeCN/H_2O, 0.1% TFA) as TFA salt. ^{1}H NMR (DMSO-d_6): δ 0.71 (m, 2H), 0.81 (m, 2H), 2.51 (s, 3H), 3.04 (m, 1H), 7.45 (d, J = 8.1 Hz, 1H), 7.45 (d, J = 8.1 Hz, 1H), 7.85 (dd, J = 7.9, 1.8 Hz, 1H), 7.90 (d, J = 3.2 Hz, 2H), 8.15 (dd, J = 8.6, 2.4 Hz, 1H), 8.25 (d, J = 1.6 Hz, 1H), 8.38 (d, J = 2.5 Hz, 1H), 8.46 (s, 1H), 8.76 (s, 1H), 10.67 (s, 1H). MS $[M + H]^+$ 512.7. Anal. calcd for ($C_{25}H_{20}ClF_3N_6O \cdot 1.4 CF_3CO_2H$): C, H, N.

(*E*)-3-(2-(6-(Cyclopropylamino)-9*H*-purin-9-yl)vinyl)-4-methyl-*N*-(3-(*tert*-butyl)phenyl)benzamide (9d). Method B; purified by reverse phase prep-HPLC (MeCN/H_2O, 0.1% TFA) as TFA salt. ^{1}H NMR (DMSO-d_6): δ 0.71 (m, 2H), 0.81 (m, 2H), 1.31 (s, 9H), 2.51 (s, 3H), 3.06 (m, 1H), 7.15 (m, 1H), 7.29 (dd, J = 7.9, 7.9 Hz, 1H), 7.42 (d, J = 8.0 Hz, 1H), 7.69 (m, 1H), 7.79 (dd, J = 1.9, 1.9 Hz, 1H), 7.84 (dd, J = 7.6, 1.7 Hz, 1H), 7.91 (d, J = 3.8 Hz, 2H), 8.24 (d, J = 1.4 Hz, 1H), 8.45 (s, 1H), 8.75 (s, 1H), 10.21 (s, 1H). MS $[M + H]^+$ 466.7. Anal. calcd for ($C_{28}H_{30}N_6O \cdot 1.2CF_3CO_2H$): C, H, N.

(*E*)-3-(2-(6-(Cyclopropylamino)-9*H*-purin-9-yl)vinyl)-4-methyl-*N*-(3-(*iso*-propyl)phenyl)benzamide (9e). Method B; purified by reverse phase prep-HPLC (MeCN/H_2O, 0.1% TFA) as TFA salt. ^{1}H NMR (DMSO-d_6): δ 0.71 (m, 2H), 0.80 (m, 2H), 1.23 (d, J = 6.9 Hz, 6H), 2.51 (s, 3H), 2.89 (septet, J = 6.9 Hz, 1H), 3.06 (m, 1H), 7.00 (d, J = 7.6 Hz, 1H), 7.28 (dt, J = 2.5, 7.8 Hz, 1H), 7.42 (d, J = 8.0 Hz, 1H), 7.65 (m, 2H), 7.83 (dd, J = 2.0, 1.7 Hz, 1H), 7.90(s, 1H), 7.92 (s, 1H), 8.24 (d, J = 1.5 Hz, 1H), 8.45 (s, 1H), 8.75 (s, 1H), 10.21 (s, 1H). MS $[M + H]^+$ 452.7.

(*E*)-3-(2-(6-(Cyclopropylamino)-9*H*-purin-9-yl)vinyl)-4-methyl-*N*-(5-(*tert*-butyl)thiazo-2-yl)benzamide (9f). Method B. ^{1}H NMR ($CDCl_3$): δ 0.70 (m, 2H), 0.89 (m, 2H), 1.31 (s, 9H), 2.53 (s, 3H), 3.09 (m, 1H), 6.01 (s, 1H), 6.61 (s, 1H), 7.38 (d, J = 8.0 Hz, 1H), 7.61 (d, J = 14.6 Hz, 1H), 7.78 (d, J = 14.9 Hz, 1H), 7.82 (dd, J = 8.0, 1.9 Hz, 1H), 8.06 (s, 1H), 8.17 (d, J = 1.6 Hz, 1H), 8.56 (s, 1H). Anal. calcd for ($C_{25}H_{27}N_7OS$): C, H, N.

(*E*)-3-(2-(6-(Cyclopropylamino)-9*H*-purin-9-yl)vinyl)-4-methyl-*N*-(5-(*tert*-butyl)oxazo-3-yl)benzamide (9g). Method B. ^{1}H NMR ($CDCl_3$): δ 0.75 (m, 2H), 0.98 (m, 2H), 1.39 (s, 9H), 2.52 (s, 3H), 3.15 (m, 1H), 6.62 (br, 1H), 6.88 (s, 1H), 7.27−7.52 (m, 2H), 7.66 (m, 1H), 8.00 (m, 1H), 8.05 (d, J = 18.8 Hz, 1H), 8.49 (s, 1H), 9.31 (s, 1H).

(*E*)-3-(2-(6-(Cyclopropylamino)-9*H*-purin-9-yl)vinyl)-4-methyl-*N*-(1-methyl-3-(*tert*-butyl)pyrazo-5-yl)benzamide (9h). Method B; purified by reverse phase prep-HPLC (MeCN/H_2O, 0.1% TFA) as TFA salt. ^{1}H NMR (DMSO-d_6): δ 0.71 (m, 2H), 0.80 (m, 2H), 1.27 (s, 9H), 2.51 (s, 3H), 3.06 (m, 1H), 3.64 (s, 3H), 6.11 (s, 1H), 7.43 (d, J = 8.0 Hz, 1H), 7.82 (dd, J = 8.0, 1.6 Hz, 1H), 7.84 (d, J = 14.8 Hz, 1H), 7.89 (d, J = 10.4 Hz, 1H), 7.93 (d, J = 14.7 Hz, 1H), 8.26 (s, 1H), 8.44 (s, 1H), 8.78 (s, 1H), 10.29 (s, 1H). MS $[M + H]^+$ 470.7. Anal. calcd for ($C_{26}H_{30}N_8O \cdot 2 CF_3CO_2H$): C, H, N.

(*E*)-3-(2-(6-(Cyclopropylamino)-9*H*-purin-9-yl)vinyl)-4-methyl-*N*-(4-(trifluoromethyl)pyridin-2-yl)benzamide (9i). Method B; 82% yield, white solid, mp 232 °C. ^{1}H NMR (DMSO-d_6, 300 MHz): δ 11.44 (s, 1H), 8.72 (s, 1H), 8.69 (s, 1H), 8.59 (s, 1H), 8.38 (m, 2H), 8.05 (m, 1H), 8.03 (d, 1H, J=14.7 Hz), 7.87 (d, 1H, J=7.9 Hz), 7.81 (d, 1H, J=14.7 Hz), 7.55 (d, 1H, J=4.1 Hz), 7.42 (d, 1H, J=8.0 Hz), 3.09 (m, 1H), 2.43 (s, 3H), 0.74 (m, 2H), 0.66 (m, 2H). MS $[M+H]^+$ 480.0 Anal. calcd for ($C_{24}H_{20}F_3N_7O$): C, H, N.

***N*-(3-Iodo-4-methylphenyl)-*N*′-(3-(trifluoromethyl)phenyl)urea (10).** A mixture of 3-(trifluoromethyl)phenylisocyanate (1.03 g, 5.5 mmol) and 3-iodo-4-methylaniline (1.17 g, 5 mmol) in CH_2Cl_2 (20 mL) was stirred at rt for 4 h. Filtration gave pure product as white solid, 98% yield. ^{1}H NMR (DMSO-d_6): δ 2.31 (s, 3H), 7.22−7.33 (m, 3H), 7.48−7.59 (m, 2H), 8.00 (s, 1H), 8.09 (d, J = 2.0 Hz, 1H), 8.80 (s, 1H), 9.03 (s, 1H).

(*E*)-1-(3-(2-(6-(Cyclopropylamino)-9*H*-purin-9-yl)vinyl)-4-methylphenyl)-3-(3-(trifluoromethyl)phenyl)urea (11). Method B. ^{1}H NMR (CD_3OD): δ 0.67 (m, 2H), 0.89 (m, 2H), 2.39 (s, 3H), 2.98 (m, 1H), 7.12−7.33 (m, 3H), 7.46 (m, 1H), 7.58−7.80 (m, 4H), 7.93 (s, 1H), 8.37 (s, 1H), 8.44 (s, 1H).

(*E*)-3-(2-(6-(Cyclopropylamino)-9*H*-purin-9-yl)vinyl)-4-methyl-*N*-(3-(4-methyl-1-imidazol-1-yl)-5-(trifluoromethyl)phenyl)benzamide (14a). Method B. ^{1}H NMR (DMSO-d_6): δ 0.66 (m, 2H), 0.74 (m, 2H), 2.19 (s, 3H), 2.50 (s, 3H), 3.29 (m, 1H), 7.45 (d, J = 8.1 Hz, 1H), 7.50 (s, 1H), 7.74 (s, 1H), 7.86 (dd, J = 7.9, 1.6 Hz, 1H), 7.90 (d, J = 1.3 Hz, 2H), 8.16−8.21 (m, 2H), 8.27 (d, J = 1.3 Hz, 1H), 8.33−8.39 (m, 2H), 8.67 (s, 1H), 10.71 (s, 1H). MS $[M + H]^+$ 558.8. Anal. calcd for ($C_{29}H_{25}F_3N_8O \cdot 0.09CH_2Cl_2$): C, H, N.

3-Iodo-4-methyl-*N*-[3-(imidazol-1-yl)-5-(trifluoromethyl)phenyl]-benzamide (13b). Prepared via our previously reported procedure for the synthesis of **13a**.[29] ^{1}H NMR (DMSO-d_6): 2.47 (s, 3H), 7.28 (s, 1H), 7.59 (d, J = 8.0 Hz, 1H), 7.84 (s, 2H), 7.95 (d, J = 7.9 Hz, 1H), 8.22 (s, 1H), 8.33 (s, 1H), 8.36 (s, 1H), 8.50 (s, 1H), 10.71 (s, 1H).

(*E*)-3-(2-(6-(Cyclopropylamino)-9*H*-purin-9-yl)vinyl)-4-methyl-*N*-(3-(1*H*-imidazol-1-yl)-5-(trifluoromethyl)phenyl)benzamide (14b). Method B. ^{1}H NMR (DMSO-d_6): 0.67 (m, 2H), 0.76 (m, 2H), 2.50 (s, 3H), 3.67 (m, 1H), 7.44 (d, J = 8.0 Hz, 2H),

7.84−7.92 (m, 4H), 8.06 (d, J = 8.1 Hz, 2H), 8.26 (s, 1H), 8.29 (d, J = 16.8 Hz, 2H), 8.39 (s, 1H), 8.67 (s, 1H), 10.62 (s, 1H). MS $[M + H]^+$ 545.1.

5-(4-Morpholinyl)-3-(trifluoromethyl)benzenamine (15a). A suspension of 3-bromo-5-(trifluoromethyl)aniline (3.0 g, 12.5 mmol), *N*-methylpiperazine (5.55 g, 50 mmol), and CsOH monohydrate (4.20 g, 25 mmol) in DMSO (48 mL) was heated at 120 °C in a sealed tube for 4 h. DMSO was then removed under vacuum. The residue was suspended in CH_2Cl_2, and the inorganic salts were filtered off. The filtrate was concentrated on rotavap and then subjected to silica gel column chromatography (5% MeOH/CH_2Cl_2), yielding the desired product as pale-yellow oil. ^{1}H NMR ($CDCl_3$): δ 3.23 (m. 4H), 3.92 (m, 4H), 6.35 (s, 1H), 6.45 (s, 1H), 6.56 (s, 1H).

3-(4-Methyl-1-piperazinyl)-5-(trifluoromethyl)benzenamine (15b). ^{1}H NMR ($CDCl_3$): δ 2.34 (s, 3H), 2.65 (m, 4H), 3.30 (m, 4H), 3.79 (br, 2H), 6.31 (s, 1H), 6.39 (s, 1H), 6.51 (s, 1H).

3-Iodo-4-methyl-*N*-[3-(morpholin-4-yl)-5-(trifluoromethyl)phenyl]-benzamide (16a). Method D. ^{1}H NMR (DMSO-d_6): 3.21 (m, 4H), 3.78 (m, 4H), 7.01 (s, 1H), 7.50 (d, J = 8.0 Hz, 1H), 7.67 (s, 1H), 7.69 (s, 1H), 7.98 (d, J = 7.9 Hz, 1H), 8.41 (s, 1H), 10.31 (s, 1H).

3-Iodo-4-methyl-*N*-[3-(4-methylpiperazin-1-yl)-5-(trifluoromethyl)-phenyl]benzamide (16b). Method D. ^{1}H NMR (DMSO-d_6): 2.23 (s, 3H), 2.46 (s, 3H), 2.50 (m, 4H), 3.27 (m, 4H), 6.97 (s, 1H), 7.54 (d, J = 8.0 Hz, 1H), 7.64 (s, 1H), 7.66 (s, 1H), 7.94 (d, J = 7.9 Hz, 1H), 8.33 (s, 1H), 10.29 (s, 1H).

(*E*)-3-(2-(6-(Cyclopropylamino)-9*H*-purin-9-yl)vinyl)-4-methyl-*N*-[3-(morpholin-4-yl)-5-(trifluoromethyl)phenyl]benzamide (17a). Method B. ^{1}H NMR (DMSO-d_6): 0.67 (m, 2H), 0.73 (m, 2H), 2.49 (s, 3H), 3.14 (m, 1H), 3.21 (t, J = 4.6 Hz, 2H), 3.77 (t, J = 4.6 Hz, 2H), 6.98 (s, 1H), 7.43 (d, J = 8.0 Hz, 1H), 7.70 (m, 2H), 7.83 (d, J = 7.71, 1H), 7.91 (s, 1H), 7.93 (d, J = 15.5 Hz, 1H), 8.05 (d, J = 3.5 Hz, 1H), 8.24 (s, 1H), 8.39 (s, 1H), 8.66 (s, 1H), 10.39 (s, 1H). MS $[M + H]^+$ 564.1. Anal. calcd for ($C_{29}H_{28}F_3N_7O_2$): C, H, N.

(*E*)-3-(2-(6-(Cyclopropylamino)-9*H*-purin-9-yl)vinyl)-4-methyl-*N*-[3-(4- methylpiperazin- 1-yl)-5-(trifluoromethyl)phenyl]benzamide (17b). Method B. ^{1}H NMR (DMSO-d_6): 0.68 (m, 2H), 0.77 (m, 2H), 2.36 (s, 3H), 2.50 (s, 3H), 2.60 (m, 4H), 3.25 (m, 4H), 4.05 (m, 1H), 7.01 (s, 1H), 7.42 (d, J = 8.1 Hz, 1H), 7.86 (d, J = 14.8 Hz, 1H), 7.81 − 7.91 (m, 4H), 8.04 (br, 1H), 8.24 (s, 1H), 8.38 (s, 1H), 8.66 (s, 1H), 10.57 (s, 1H). MS $[M + H]^+$ 577.1.

(*E*)-3-(2-(Purin-9-yl)vinyl)-4-methyl-*N*-(3-(4-methyl-1-imidazol-1-yl)-5-(trifluoromethyl)phenyl)benzamide (18a). Method B. ^{1}H NMR (DMSO-d_6): 2.19 (s, 3H), 2.50 (s, 3H), 7.49 (d, J = 8.3 Hz, 1H), 7.50 (s, 1H), 7.75 (s, 1H), 7.89 (d, J = 7.9 Hz, 1H), 8.02 (d, J = 3.1 Hz, 2H), 8.19 (d, J = 17.1 Hz, 2H), 8.32 (d, J = 6.8 Hz, 2H), 9.11 (s, 2H), 9.29 (s, 1H), 10.72 (s, 1H). MS $[M + H]^+$ 503.9. Anal. calcd for ($C_{26}H_{20}F_3N_7O$): C, H, N.

(*E*)-3-(2-(Purin-9-yl)vinyl)-4-methyl-*N*-(4-(trifluoromethyl)pyridin-2-yl)benzamide (18b). Method B. ^{1}H NMR (DMSO-d_6): 2.73 (s, 1.5H), 2.89 (s, 1.5H), 7.43 (d, J = 8.0 Hz, 1H), 7.54 (d, J = 4.3 Hz, 1H), 7.88−7.94 (m, 2H), 8.13 (d, J = 14.7 Hz, 1H), 8.40 (s, 1H), 8.59 (s, 1H), 8.70 (d, J = 4.7 Hz, 1H), 9.10 (s, 1H), 9.14 (s, 1H), 9.28 (s, 1H), 11.41 (s, 1H). MS $[M + H]^+$ 424.9. Anal. calcd for ($C_{21}H_{15}F_3N_6O \cdot 0.15CH_2Cl_2$): C, H, N.

Modeling Studies. The binding site model used for Abl docking was based on the X-ray coordinates of Abl bound with an imatinib derivative, PDB-ID 1fpu. Protein side chains within a 5 Å radius of the bound ligand were allowed to relax to optimize binding interactions using the Induced Fit protocol in the Schrodinger package.[24] The binding site model used for Src docking was based on a homology model of Src built from the crystal structure of Lck bound with a DFG-out inhibitor (2og8)[34] using Prime in the Schrodinger package. Docking studies were performed with Glide in the Schrodinger modeling package.[24] The solution with the best docking score was chosen and used for analysis.

Wild Type Abl, Abl T315I, and Src LANCE Assay. Inhibition of wild type Abl, Abl T315I, or Src activity was measured in a homogeneous time-resolved fluorescence resonance energy transfer (TR-FRET) assay using purified human wild-type Abl kinase (Panvera), Abl T315I (Upstate Biotechnology Inc.), or partially purified human Src (Upstate Biotechnology Inc.), and biotinylated phosphokinase substrate peptides: Biotin-EKKMAAEAIYAAPFAK-NH_2 (Quality Controlled Biochemicals) for wild type Abl and Abl T315I, and Biotin-KVEKIGEGTYGVVYK-NH_2 (Pierce) for Src. The kinase reactions were carried out in complete LANCE kinase buffer (LKB) and consisted of 20 mM NaHEPES pH 7.4, 0.1 mg/mL BSA, 1 mM ATP, 10 mM $MgCl_2$, and 0.41 mM DTT in round-bottom black 96-well Microfluor plates (Dynex Technologies Inc.) preblocked with 1% BSA in PBS at 4 °C overnight. For the kinase reaction, compound dilutions were incubated with wild type Abl or Abl T315I (40 pM) or Src (165 pM) and their substrate peptide (50 nM) 1 h for Abl T315I or 2 h for Abl at room temperature, or 2 h at 37 °C for Src, in a total volume of 0.1 mL LKB. The kinase reaction was terminated by addition of 0.05 mL of a kill/detection solution containing 15 μM of a potent ARIAD kinase inhibitor, 6 nM europium-labeled anti-phosphotyrosine mAb PT66 and 60 nM allophycocyanin-labeled streptavidin (LANCE reagents from Perkin-Elmer Inc.). Assay plates were incubated at room temperature in the dark for 20 min prior to reading fluorescence at 615 and 665 nm on a Victor2 V plate reader (Perkin-Elmer). Positive and negative controls and a standard curve for phosphorylated peptide were included on each plate. Data values were transferred to an Excel spreadsheet and IC_{50}s were calculated from the fluorescence at 665 nm by interpolation between the averaged duplicate well data on 3-fold serial dilutions of test inhibitor.

Proliferation Assay. K562 human wild-type Bcr-Abl CML cell line and murine pro-B Ba/F3 cell line stably transfected with constructs expressing full-length wild-type Bcr-Abl or Bcr-Abl with various kinase domain point mutations (T315I, L248R, G250E, Q252H, Y253H, and E255K) were used in the cell proliferation assays. The parental Ba/F3 cell line was used as control. K562 cell line was obtained from the American Type Culture Collection (ATCC) and maintained in Iscove's modified Dulbecco's medium with 10% FBS. Ba/F3 cell lines were kindly provided by Brian J. Druker (Howard Hughes Medical Institute, Oregon Health and Science University, Portland, OR) and were maintained in RPMI 1640 growth medium with 10% FBS except the parental Ba/F3 cell line, which was maintained in the same medium supplemented with 10 ng/mL IL-3. All cells were incubated at 37 °C in 5% CO_2. After the compounds were incubated with the cells for 3 days, the number of viable cells in each well in 96-well plate was measured using an MTS assay (Promega). MTS reagent was added to all wells and then the plates were returned to the incubator at 37 °C for 2 h. The absorbance in each well was then measured at 490 nm using a Wallac Victor^{2}V plate reader. The IC_{50} was calculated by determining the concentration of compound required to decrease the MTS signal by 50% in best-fit curves using Microsoft XLfit software and comparing with baseline, the DMSO control, as 0% inhibition.

Pharmacokinetics (PK) and in Vivo Efficacy. All in vivo experiments were conducted in accordance with ARIAD Pharmaceuticals, Inc. Institutional Animal Care and Use Committee (IACUC) guidelines. Unless otherwise stated, all animals were obtained from Charles River Laboratories (Wilmington, MA). Rats were housed two per cage and mice were housed five per cage, were in micro isolator caging, and were offered food and water ad libitum unless otherwise stated.

PK Studies. Oral and intravenous pharmacokinetic testing was performed on CD rats. For oral dosing, the rats were fasted overnight and received food 2 h post dosing. Each rat was dosed according to each individual body weight measured just prior to dose administration. The dosing levels and volumes were set at 15 mg/kg and 4 mL for po administration and 5 mg/kg and

2 mL for iv administration. Blood was collected into microcentrifuge tubes containing a small amount of 5 mM EDTA from the retro orbital plexus of each rat at prescribed time points, the tubes were centrifuged, and plasma was isolated for LC-MS analysis.

As a prerequisite to evaluating in vivo efficacy, some compounds were subjected to oral pharmacokinetic testing on mice. The animals were not fasted and were dosed at a fixed volume of 10 mL and three different levels (10, 30, and 100 mg/kg) for the purpose of observing dose response. Blood was collected from three mice at each time point via exsanguination.

In Vivo Efficacy Studies. (1) Ba/F3 WT Bcr-Abl survival model: Ba/F3 cell line expressing wild type Bcr-Abl was kindly provided by Brian J. Druker (Howard Hughes Medical Institute, Oregon Health and Science University, Portland, OR). Eight to ten week old female CB17 SCID mice were injected intravenously with 1×10^6 cells per mouse on day zero and randomly selected into groups ($n = 10$). Treatments began on day three after cell injection and were administered daily for up to 21 consecutive days. Mice were observed twice daily during the week and once daily during the weekend. Animals were euthanized via CO_2 asphyxiation when they became moribund according to the company IACUC guidelines. Mice dead of disease were verified showing splenomegaly at necropsy. Percent survival refers to the percentage of mice remaining "on-study" at the end of the day. (2) Src Y527F mouse tumor model: A c-Src Y527F overexpressing cell line was established from NIH3T3 mouse fibroblasts transformed with a mutant chicken Src (Y527F). It was kindly provided by Dr. David Shalloway at Cornell University. Eight to ten week old female CD-1 nude mice were injected subcutaneously with 2×10^6 cells per mouse and were randomly selected into treatment groups ($n = 10$) when the average tumor size was ~200 mm^3 (day zero). Treatments were administered orally for 21 consecutive days. Subcutaneous tumors were measured 2 or 3 times weekly. Tumor volume (in mm^3) was calculated using the formula $(L \times W^2)/2$. When a tumor reached 10% of the body weight of the host, the animal was euthanized via CO_2 asphyxiation.

Supporting Information Available: Combustion analysis of certain tested compounds. This material is available free of charge via the Internet at http://pubs.acs.org.

References

(1) Nowell, P. C.; Hungerford, D. A. A minute chromosome in chronic granulocytic leukemia. *Science* **1960**, *132*, 1497–1501.

(2) (a) Rowley, J. D. A new consistent chromosomal abnormality in chronic myelogenous leukemia identified by quinacrine fluorescence and Giemsa staining. *Nature* **1973**, *243*, 290–293. (b) Groffen, J; Stephenson, J. R.; Heisterkamp, N.; de Klein, A.; Bartram, C. R.; Grosveld, G. Philadelphia chromosomal breakpoints are clustered within a limited region, bcr, on chromosome 22. *Cell* **1984**, *36*, 93–99.

(3) (a) Lugo, T. G.; Pendergast, A. M.; Muller, A. J.; Witte, O. N. Tyrosine kinase activity and transformation potency of Bcr-Abl oncogene products. *Science* **1990**, *247*, 1079–1082. (b) Sawyers, C. L. Chronic myeloid leukemia. *N. Engl. J. Med.* **1999**, *340*, 1330–1340.

(4) Capdeville, R.; Buchdunger, E.; Zimmermann, J.; Matter, A. Glivec (STI571, imatinib), a rationally developed, targeted anticancer drug. *Nat. Rev. Drug Discovery* **2002**, *1*, 493–502.

(5) Weisberg, E.; Manley, P. W.; Cowan-Jacob, S. W.; Hochhaus, A.; Griffin, J. D. Second generation inhibitors of BCR-ABL for the treatment of imatinib-resistant chronic myeloid leukemia. *Nat. Rev. Cancer* **2007**, *7*, 345–356.

(6) (a) Shah, N. P.; Tran, C.; Lee, F. Y.; Chen, P.; Norris, D.; Sawyers, C. L. Overriding imatinib resistance with a novel Abl kinase inhibitor. *Science* **2004**, *305*, 399–402. (b) O'Hare, T.; Walters, D. K.; Stoffregen, E. P.; Jia, T.; Manley, P. W.; Mestan, J.; Cowan-Jacob, S. W.; Lee, F. Y.; Heinrich, M. C.; Deininger, M. W. N.; Druker, B. J. In vitro activity of Bcr-Abl inhibitors AMN107 and BMS-354825 against clinically relevant imatinib-resistant Abl kinase domain mutants. *Cancer Res.* **2005**, *65*, 4500–4505. (c) O'Hare, T.; Eide, C. A.; Deininger, M. W. N. Bcr-Abl kinase domain mutations, drug resistance, and the road to a cure for chronic myeloid leukemia. *Blood* **2007**, *110*, 2242–2249. (d) O'Hare, T.; Eide, C. A.; Deininger, M. W. New Bcr-Abl inhibitors in chronic myeloid leukemia: keeping resistance in check. *Exp. Opin. Invest. Drugs* **2008**, *17*, 865–878. (e) Lee, F.; Fandi, A.; Voi, M. Overcoming kinase resistance in chronic myeloid leukemia. *Int. J. Biochem. Cell Biol.* **2008**, *40*, 334–343. (f) Tanaka, R.; Kimura, S. Abl tyrosine kinase inhibitors for overriding Bcr-Abl/ T315I: from the second to third generation. *Exp. Rev. Anticancer Ther.* **2008**, *8*, 1387–1398. (g) Noronha, G.; Cao, J.; Chow, C. P.; Dneprovskaia, E.; Fine, R. M.; Hood, J.; Kang, X.; Klebansky, B.; Lohse, D.; Mak, C. C.; McPherson, A.; Palanki, M. S. S.; Pathak, V. P.; Renick, J.; Soll, R.; Zeng, B. Inhibitors of ABL and the ABL- T315I mutation. *Curr. Top. Med. Chem* **2008**, *8*, 905–921. (h) Quintas-Cardama, A.; Cortes, J. Therapeutic options against BCR-ABL1 T315I -positive chronic myelogenous leukemia. *Clin. Cancer Res.* **2008**, *14*, 4392–4399.

(7) (a) Mahon, F.-X.; Hayette, S.; Lagarde, V.; Belloc, F.; Turcq, B.; Nicolini, F.; Belanger, C.; Manley, P. W.; Leroy, C.; Etienne, G.; Roche, S.; Pasquet, J.-M. Evidence that resistance to nilotinib may be due to Bcr-Abl, Pgp, or Src kinase overexpression. *Cancer Res.* **2008**, *68*, 9809–9816. (b) Schenone, S.; Manetti, F.; Botta, M. Last findings on dual inhibitors of Abl and Src tyrosine-kinases. *Mini-Rev. Med. Chem.* **2007**, *7*, 191–201. (c) Kantarjian, H. M.; Giles, F.; Quintas-Cardama, A.; Cortes, J. Important therapeutic targets in chronic myelogenous leukemia. *Clin. Cancer Res.* **2007**, *13*, 1089–1097. (d) Martinelli, G.; Soverini, S.; Rosti, G.; Baccarani, M. Dual tyrosine kinase inhibitors in chronic myeloid leukemia. *Leukemia* **2005**, *19*, 1872–1879.

(8) Hu, Y.; Liu, Y.; Pelletier, S.; Buchdunger, E.; Warmuth, M.; Fabbro, D.; Hallek, M.; Van Etten, R. A.; Li, S. Requirement of Src kinases Lyn, Hck and Fgr for *BCR-ABL1*-induced B-lymphoblastic leukemia but not chronic myeloid leukemia. *Nat. Genet.* **2004**, *36*, 453–461.

(9) (a) Srinivasan, D.; Plattner, R. Activation of Abl tyrosine kinases promotes invasion of aggressive breast cancer cells. *Cancer Res.* **2006**, *66*, 5648–5655. (b) Srinivasan, D.; Sims, J. T.; Plattner, R. Aggressive breast cancer cells are dependent on activated Abl kinases for proliferation, anchorage-independent growth and survival. *Oncogene* **2008**, *27*, 1095–1105.

(10) Lin, J.; Arlinghaus, R. Activated c-Abl tyrosine kinase in malignant solid tumors. *Oncogene* **2008**, *27*, 4385–4391.

(11) (a) Park, S. I.; Shah, A. N.; Zhang, J.; Gallick, G. E. Regulation of angiogenesis and vascular permeability by Src family kinases: opportunities for therapeutic treatment of solid tumors. *Expert Opin. Ther. Targets* **2007**, *11*, 1207–1217. (b) Summy, J. M.; Gallick, G. E. Treatment for advanced tumors: Src reclaims center stage. *Clin. Cancer Res.* **2006**, *12*, 1398–1401. (c) Chen, T.; George, J. A.; Taylor, C. C. Src tyrosine kinase as a chemotherapeutic target: is there a clinical case?. *Anti-Cancer Drugs* **2006**, *17*, 123–131. (d) Alvarez, R. H.; Kantarjian, H. M.; Cortes, J. E. The role of Src in solid and hematologic malignancies: development of new-generation Src inhibitors. *Cancer* **2006**, *107*, 1918–1929. (e) Lesslie, D. P.; Gallick, G. E. Src family kinases as regulators of angiogenesis: therapeutic implications. *Curr. Cancer Ther. Rev.* **2005**, *1*, 45–50. (f) Tsygankov, A. Y.; Shore, S. K. Src: regulation, role in human carcinogenesis and pharmacological inhibitors. *Curr. Pharm. Des.* **2004**, *10*, 1745–1756. (g) Yeatman, T. J. A renaissance for Src. *Nat. Rev. Cancer* **2004**, *4*, 470–480.

(12) Lombardo, L. J.; Lee, F. Y.; Chen, P.; Norris, D.; Barrish, J. C.; Behnia, K.; Castaneda, S.; Cornelius, L. A. M.; Das, J.; Doweyko, A. M.; Fairchild, C.; Hunt, J. T.; Inigo, I.; Johnston, K.; Kamath, A.; Kan, D.; Klei, H.; Marathe, P.; Pang, S.; Peterson, R.; Pitt, S.; Schieven, G. L.; Schmidt, R. J.; Tokarski, J.; Wen, M.-L.; Wityak, J.; Borzilleri, R. M. Discovery of *N*-(2-chloro-6-methyl-phenyl)-2-(6-(4-(2-hydroxyethyl)-piperazin-1-yl)-2-methylpyrimidin-4-ylamino)thiazole-5-carboxamide (BMS-354825), a dual Src/Abl kinase inhibitor with potent antitumor activity in preclinical assays. *J. Med. Chem.* **2004**, *47*, 6658–6661.

(13) (a) Boschelli, D. H.; Ye, F.; Wang, Y. D.; Dutia, M.; Johnson, S. L.; Wu, B.; Miller, K.; Powell, D. W.; Yaczko, D.; Young, M.; Tischler, M.; Arndt, K.; Discafani, C.; Etienne, C.; Gibbons, J.; Grod, J.; Lucas, J.; Weber, J. M.; Boschelli, F. Optimization of 4-phenylamino-3-quinolinecarbonitriles as potent inhibitors of Src kinase activity. *J. Med. Chem.* **2001**, *44*, 3965–3977. (b) Hennequin, L. F.; Allen, J.; Breed, J.; Curwen, J.; Fennell, M.; Green, T. P.; Lambert-van der Brempt, C.; Morgentin, R.; Norman, R. A.; Olivier, A.; Otterbein, L.; Ple, P. A.; Warin, N.; Costello, G. *N*-(5-Chloro-1,3-benzodioxol-4-yl)-7-[2-(4-methylpiperazin-1-yl)ethoxy]-5-(tetrahydro-2*H*-pyran-4-yloxy)quinazolin-4-amine, a novel, highly

selective, orally available, dual-specific c-Src/Abl kinase inhibitor. *J. Med. Chem.* **2006**, *49*, 6465–6488.
(14) Fabian, M. A.; Biggs, W. H.; Treiber, D. K.; Atteridge, C. E.; Azimioara, M. D.; Benedetti, M. G.; Carter, T. A.; Ciceri, P.; Edeen, P. T.; Floyd, M.; Ford, J. M.; Galvin, M.; Gerlach, J. L.; Grotzfeld, R. M.; Herrgard, S.; Insko, D. E.; Insko, M. A.; Lai, A. G.; Lelias, J.-M.; Mehta, S. A.; Milanov, Z. V.; Velasco, A. M.; Wodicka, L. M.; Patel, H. K.; Zarrinkar, P. P.; Lockhart, D. J. A small molecule−kinase interaction map for clinical kinase inhibitors. *Nat. Biotechnol.* **2005**, *23*, 329–336.
(15) (a) Schindler, T.; Bornmann, W.; Pellicena, P.; Miller, W. T.; Clarkson, B.; Kuriyan, J. Structural mechanism for STI-571 inhibition of Abelson tyrosine kinase. *Science* **2000**, *289*, 1938–1942. (b) Mol, C. D.; Fabbro, D.; Hosfield, D. J. Structural insights into the conformational selectivity of STI-571 and related kinase inhibitors. *Curr. Opin. Drug Discovery Dev.* **2004**, *7*, 639–648.
(16) (a) Weisberg, E.; Manley, P. W.; Breitenstein, W.; Brueggen, J.; Cowan-Jacob, S. W.; Ray, A.; Huntly, B.; Fabbro, D.; Fendrich, G.; Hall-Meyers, E.; Kung, A. L.; Mestan, J.; Daley, G. Q.; Callahan, L.; Catley, L.; Cavazza, C.; Mohammed, A.; Neuberg, D.; Wright, R. D.; Gilliland, D. G.; Griffin, J. D. Characterization of AMN107, a selective inhibitor of native and mutant Bcr-Abl. *Cancer Cell* **2005**, *7*, 129–141. (b) Golemovic, M.; Verstovsek, S.; Giles, F.; Cortes, J.; Manshouri, T.; Manley, P. W.; Mestan, J.; Dugan, M.; Alland, L.; Griffin, J. D.; Arlinghaus, R. B.; Sun, T.; Kantarjian, H.; Beran, M. AMN107, a novel aminopyrimidine inhibitor of Bcr-Abl, has in vitro activity against imatinib-resistant chronic myeloid leukemia. *Clin. Cancer Res.* **2006**, *11*, 4941–4947. (c) Manley, P. W.; Cowan-Jacob, S. W.; Mestan, J. Advances in the structural biology, design and clinical development of Bcr-Abl kinase inhibitors for the treatment of chronic myeloid leukaemia. *Biochim. Biophys. Acta, Proteins Proteomics* **2005**, *1754*, 3–13.
(17) (a) Horio, T.; Hamasaki, T.; Inoue, T.; Wakayama, T.; Itou, S.; Naito, H.; Asaki, T.; Hayase, H.; Niwa, T. Structural factors contributing to the Abl/Lyn dual inhibitory activity of 3-substituted benzamide derivatives. *Bioorg. Med. Chem. Lett.* **2007**, *17*, 2712–2717. (b) Asaki, T.; Sugiyama, Y.; Hamamoto, T.; Higashioka, M.; Umehara, M.; Naito, H.; Niwa, T. Design and synthesis of 3-substituted benzamide derivatives as Bcr-Abl kinase inhibitors. *Bioorg. Med. Chem. Lett.* **2006**, *16*, 1421–1425. (c) Kimura, S.; Naito, H.; Segawa, H.; Kuroda, J.; Yuasa, T.; Sato, K.; Yokota, A.; Kamitsuji, Y.; Kawata, E.; Ashihara, E.; Nakaya, Y.; Naruoka, H.; Wakayama, T.; Nasu, K.; Asaki, T.; Niwa, T.; Hirabayashi, K.; Maekawa, T. NS-187, a potent and selective dual Bcr-Abl/Lyn tyrosine kinase inhibitor, is a novel agent for imatinib-resistant leukemia. *Blood* **2005**, *106*, 3948–3954.
(18) (a) Lowinger, T. B.; Riedl, B.; Dumas, J.; Smith, R. A. Design and discovery of small molecules targeting Raf-1 kinase. *Curr. Pharm. Des.* **2002**, *8*, 2269–2278. (b) Wan, P. T. C.; Garnett, M. J.; Roe, S. M.; Lee, S.; Niculescu-Duvaz, D.; Good, V. M.; Jones, C. M.; Marshall, C. J.; Springer, C. J.; Barford, D.; Marais, R. Mechanism of activation of the Raf-Erk signaling pathway by oncogenic mutations of B-Raf. *Cell* **2004**, *116*, 855–867.
(19) Pargellis, C.; Tong, L.; Churchill, L.; Cirillo, P. F.; Gilmore, T.; Graham, A. G.; Grob, P. M.; Hickey, E. R.; Moss, N.; Pav, S.; Regan, J. Inhibition of p38 Map kinase by utilizing a novel allosteric binding site. *Nat. Struct. Biol.* **2002**, *9*, 268–272.
(20) Dai, Y.; Hartandi, K.; Ji, Z.; Ahmed, A. A.; Albert, D. H.; Bauch, J. L.; Bouska, J. J.; Bousquet, P. F.; Cunha, G. A.; Glaser, K. B.; Harris, C. M.; Hickman, D.; Guo, J.; Li, J.; Marcotte, P. A.; Marsh, K. C.; Moskey, M. D.; Martin, R. L.; Olson, A. M.; Osterling, D. J.; Pease, L. J.; Soni, N. B.; Stewart, K. D.; Stoll, V. S.; Tapang, P.; Reuter, D. R.; Davidsen, S. K.; Michaelides, M. R. Discovery of *N*-(4-(3-amino-1*H*-indazol-4-yl)phenyl)-*N*′-(2-fluoro-5-methylphenyl) urea (ABT-869), a 3-aminoindazole-based orally active multitargeted receptor tyrosine kinase inhibitor. *J. Med. Chem.* **2007**, *50*, 1584–1597.
(21) (a) O'Hare, T.; Pollock, R.; Stoffregen, E. P.; Keats, J. A.; Abdullah, O. M.; Moseson, E. M.; Rivera, V. M.; Tang, H.; Metcalf, C. A.III; Bohacek, R. S.; Wang, Y.; Sundaramoorthi, R.; Shakespeare, W. C.; Dalgarno, D.; Clackson, T.; Sawyer, T. K.; Deininger, M. W.; Druker, B. J. Inhibition of wild-type and mutant Bcr-Abl by AP23464, a potent ATP-based oncogenic protein kinase inhibitor: implications for CML. *Blood* **2004**, *104*, 2532–2539. (b) Azam, M.; Nardi, V.; Shakespeare, W. C.; Metcalf, C. A.III; Bohacek, R. S.; Wang, Y.; Sundaramoorthi, R.; Sliz, P.; Veach, D. R.; Bornmann, W. G.; Clarkson, B.; Dalgarno, D. C.; Sawyer, T. K.; Daley, G. Q. Activity of dual Src-Abl inhibitors highlights the role of BCR/ABL kinase dynamics in drug resistance. *Proc. Natl. Acad. Sci. U.S.A.* **2006**, *103*, 9244–9249.
(22) Wang, Y.; Shakespeare, W. C.; Huang, W.-S.; Sundaramoorthi, R.; Lentini, S.; Das, S.; Liu, S.; Banda, G.; Wen, D.; Zhu, X.; Xu, Q.; Keats, J.; Wang, F.; Wardwell, S.; Ning, Y.; Snodgrass, J. T.; Broudy, M. I.; Russian, K.; Dalgarno, D.; Clackson, T.; Sawyer, T. K. Novel N^9-arenethenyl purines as potent dual Src/Abl tyrosine kinase inhibitors. *Bioorg. Med. Chem. Lett.* **2008**, *18*, 4907–4912.
(23) (a) Liu, Y.; Gray, N. S. Rational design of inhibitors that bind to inactive kinase conformations. *Nat. Chem. Biol.* **2006**, *2*, 358–364. (b) Okram, B.; Nagle, A.; Adrian, F. J.; Lee, C.; Ren, P.; Wang, X.; Sim, T.; Xie, Y.; Wang, X.; Xia, G.; Spraggon, G.; Warmuth, M.; Liu, Y.; Gray, N. S. A general strategy for creating "inactive-conformation" Abl inhibitors. *Chem. Biol.* **2006**, *13*, 779–786.
(24) Sherman, W.; Day, T.; Jacobson, M. P.; Friesner, R. A.; Farid, R. Novel procedure for modeling ligand/receptor induced fit effects. *J. Med. Chem.* **2006**, *49*, 534–553.
(25) Dalgarno, D.; Stehle, T.; Narula, S.; Schelling, P.; van Schravendijk, M. R.; Adams, S.; Andrade, L.; Keats, J.; Ram, M.; Jin, L.; Grossman, T.; MacNeil, I.; Metcalf, C.III; Shakespeare, W.; Wang, Y.; Keenan, T.; Sundaramoorthi, R.; Bohacek, R.; Weigele, M.; Sawyer, T. Structural basis of Src tyrosine kinase inhibition with a new class of potent and selective trisubstituted purine-based compounds. *Chem. Biol. Drug Des.* **2006**, *67*, 46–57.
(26) Boesen, T.; Madsen, C.; Henriksen, U.; Dahl, O. Preparation of *N*-(alk-1-enyl) nucleobase compounds by Horner and Horner−Wadsworth−Emmons reactions. *J. Chem. Soc., Perkin Trans. 1* **2000**, 2015–2021.
(27) Huang, W.-S.; Wang, Y.; Sundaramoorthi, R.; Thomas, R. M.; Wen, D.; Liu, S.; Lentini, S. P.; Das, S.; Banda, G.; Sawyer, T. K.; Shakespeare, W. C. Facile synthesis of 9-(arenethenyl)purines via Heck reaction of 9-vinylpurines and aryl halides. *Tetrahedron Lett.* **2007**, *48*, 7388–7391.
(28) Pitha, J.; Ts'o, P. O. P. *N*-Vinyl derivatives of substituted pyrimidines and purines. *J. Org. Chem.* **1968**, *33*, 1341–1344.
(29) Huang, W.-S.; Shakespeare, W. C. An efficient synthesis of nilotinib (AMN107). *Synthesis* **2007**, 2121–2124 and references cited therein.
(30) Pierce, A. C.; ter Haar, E.; Binch, H. M.; Kay, D. P.; Patel, S. R.; Li, P. CH···O and CH···N hydrogen bonds in ligand design: A novel quinazolin-4-ylthiazol-2-ylamine protein kinase inhibitor. *J. Med. Chem.* **2005**, *48*, 1278–1281and references cited therein .
(31) Daylight Chemical Information System, Inc. http://www.daylight.com, accessed March 2005.
(32) (a) Seeliger, M. A.; Nagar, B.; Frank, F.; Cao, X.; Henderson, M. N.; Kuriyan, J. c-Src binds to the cancer drug imatinib with an inactive Abl/c-Kit conformation and a distributed thermodynamic penalty. *Structure* **2007**, *15*, 299–311. (b) Levinson, N. M.; Kuchment, O.; Shen, K.; Young, M. A.; Koldobskiy, M.; Karplus, M.; Cole, P. A.; Kuriyan, J. A Src-like inactive conformation in the Abl tyrosine kinase domain. *PLoS Biol.* **2006**, *4*, 753–767. (c) Nagar, B.; Bornmann, W. G.; Pellicena, P.; Schindler, T.; Veach, D. R.; Miller, W. T.; Clarkson, B.; Kuriyan, J. Crystal structures of the kinase domain of c-Abl in complex with the small molecule inhibitors PD173955 and imatinib (STI-571). *Cancer Res.* **2002**, *62*, 4236–4243. (d) Cowan-Jacob, S. W.; Fendrich, G.; Manley, P. W.; Jahnke, W.; Fabbro, D.; Liebetanz, J.; Meyer, T. The crystal structure of a c-Src complex in an active conformation suggests possible steps in c-Src activation. *Structure* **2005**, *13*, 861–871.
(33) Dar, A. C.; Lopez, M. S.; Shokat, K. M. Small molecule recognition of c-Src via the Imatinib-binding conformation. *Chem. Biol.* **2008**, *15*, 1015–1022.
(34) DiMauro, E. F.; Newcomb, J.; Nunes, J. J.; Bemis, J. E.; Boucher, C.; Buchanan, J. L.; Buckner, W. H.; Cee, V. J.; Chai, L.; Deak, H. L.; Epstein, L.; Faust, T.; Gallant, P.; Geuns-Meyer, S. D.; Gore, A.; Gu, Y.; Henkle, B.; Hodous, B. L.; Hsieh, F.; Huang, X.; Kim, J. L.; Lee, J.; Martin, M. W.; Masse, C. E.; McGowan, D. C.; Metz, D.; Mohn, D.; Morgenstern, K. A.; Oliveira, dos Santos, A.; Patel, V. F.; Powers, D.; Rose, P. E.; Schneider, S.; Tomlinson, S. A.; Tudor, Y.-Y.; Turci, S. M.; Welcher, A. A.; White, R. D.; Zhao, H.; Zhu, L.; Zhu, X. Discovery of aminoquinazolines as potent, orally bioavailable inhibitors of Lck: Synthesis, SAR, and in vivo anti-inflammatory activity. *J. Med. Chem.* **2006**, *49*, 5671–5686.
(35) Azam, M. et al. Unpublished results.
(36) Wang, Y.; Huang, W.-S.; Sundaramoorthi, R.; Zhu, X.; Thomas, R. M.; Shakespeare, W. C.; Dalgarno, D. C.; Sawyer, T. K. Preparation of purine heterocyclic derivatives as kinase inhibitors for therapeutic use as anticancer agents. PCT Int. Appl. WO 2007021937, 2007.